(2)

Extracting the Shape and Roughness of Specular Lobe Objects Using Four Light Photometric Stereo

Fredric Solomon[1] and Katsushi Ikeuchi

CMU-RI-TR-91-17

The Robotics Institute
Carnegie Mellon University
Pittsburgh, Pennsylvania 15213-3890

October 31, 1991

[1] Fredric Solomon is employed by the IBM Corporation, Hopewell Junction, N.Y.

This research was sponsored by the Avionics Laboratory, Wright Research and Development Center, Aeronautical System Division (AFSC), U.S. Air Force, Wright-Patterson AFB, Ohio 45433-6543, under contract F33615-90-C-1465, ARPA order no. 7597.

REPORT DOCUMENTATION PAGE

Form Approved
OMB No. 0704-0188

1. AGENCY USE ONLY (Leave blank)	2. REPORT DATE	3. REPORT TYPE AND DATES COVERED
	October 1991	technical

4. TITLE AND SUBTITLE

Extracting the Shape and Roughness of Specular Lobe Objects Using Four Light Photometric Stereo

5. FUNDING NUMBERS

F333615-90-C-1465

6. AUTHOR(S)

F. Solomon and K. Ikeuchi

7. PERFORMING ORGANIZATION NAME(S) AND ADDRESS(ES)

The Robotics Institute
Carnegie Mellon University
Pittsburgh, PA 15213

8. PERFORMING ORGANIZATION REPORT NUMBER

CMU-RI-TR-91-17

9. SPONSORING / MONITORING AGENCY NAME(S) AND ADDRESS(ES)

Avionics Laboratory, Wright R&D Center

10. SPONSORING / MONITORING AGENCY REPORT NUMBER

11. SUPPLEMENTARY NOTES

12a. DISTRIBUTION AVAILABILITY STATEMENT

Approved for public release;
Distribution unlimited

12b. DISTRIBUTION CODE

13. ABSTRACT (Maximum 200 words)

Two important aspects of part inspection are the measurement or surface shape and surface roughness. We propose a noncontact method of measuring surface shape and surface roughness. The method, which we call "four light photometric stereo," uses four lights which sequentially illuminate the object under inspection, and a video camera for taking images of the object. Conceptually, the problem we are solving has three parts: shape extraction, pixel segmentation, and roughness extraction. The shape information is produced directly by three light and four light photometric stereo methods. After we have shape information, we can apply statistical segmentation techniques to determine which pixels are specular and which are nonspecular. Then, we can use the specular pixels and shape information, in conjugation with the simplified Torrance-Sparrow reflectance model to determine the surface roughness. The method has successfully been applied to a number of synthetic and real objects.

14. SUBJECT TERMS	15. NUMBER OF PAGES
	41 pp
	16. PRICE CODE

17. SECURITY CLASSIFICATION OF REPORT	18. SECURITY CLASSIFICATION OF THIS PAGE	19. SECURITY CLASSIFICATION OF ABSTRACT	20. LIMITATION OF ABSTRACT
unlimited	unlimited	unlimited	unlimited

Contents

Abstract

Two important aspects of part inspection are the measurement of surface shape and surface roughness. We propose a noncontact method of measuring surface shape and surface roughness. The method, which we call "four light photometric stereo", uses four lights which sequentially illuminate the object under inspection, and a video camera for taking images of the object. Conceptually, the problem we are solving has three parts: shape extraction, pixel segmentation, and roughness extraction. The shape information is produced directly by three light and four light photometric stereo methods. After we have shape information, we can apply statistical segmentation techniques to determine which pixels are specular and which are nonspecular. Then, we can use the specular pixels and shape information, in conjugation with the simplified Torrance-Sparrow reflectance model to determine the surface roughness. The method has successfully been applied to a number of synthetic and real objects.

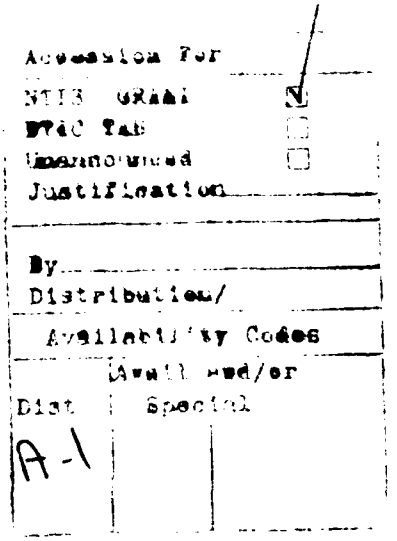

1. Introduction

In modern manufacturing environments, part inspection is an important part of quality control. Today, the majority of inspection tasks are performed manually. Manual inspection is subject to human error, is monotonous, and is very labor intensive. In an effort to automate part inspection, some companies have turned to computer vision techniques. However, these efforts have predominately been limited to two dimensional measurement. Two dimensional measurement, while not easy, is much simpler than three dimensional measurement. This is because conventional cameras see in two dimensions. Complex algorithms are required to convert a camera's two dimensional view into three dimensions. However, the ability to measure parts in three dimensions would be an important tool for inspecting manufactured parts. Two basic three dimensional measurements that are made on many manufactured parts are the measurement of the shape and surface roughness of the part.

Computer vision research has produced a number of basic techniques for measuring the surface shape of an object: stereo vision, range finders, and photometric techniques. Photometric techniques use image intensity to determine shape. There are two basic photometric techniques for transforming from image intensity to shape: experimentally derived reflectance map techniques and physically based theoretical reflectance models.

A reflectance map contains a transformation between surface orientation and image brightness for a given material, light source (direction and intensity), and viewing direction. Silver [1] described how to experimentally determine a reflectance map. In order to construct a reflectance map, a sphere needs to be constructed of the material to be inspected. Then, an image of the sphere, which contains all surface orientations, is taken with the specified lighting and viewing geometries. The reflectance map is constructed from this image. Experimentally derived reflectance maps are basically lookup tables between image intensity and surface orientation. If the material, lighting, or viewing geometries changes, a new calibrating image needs to be taken, and a new reflectance map has to be calculated.

Physically based reflectance models [2] express the relationship between image brightness, imaging geometry, lighting geometry, and surface shape in the form of an explicit mathematical function. Since the parameters of the reflectance model are expressed as a function, imaging and lighting geometries can be changed without the recalibration required by the experimentally derived reflectance map technique. There are three basic categories of reflectance models, based on surface type. Diffuse surfaces follow the lambertian reflectance model. The intensity of a lambertian surface is only dependent on the angle between the light source direction and the surface orientation. Shiny surfaces follow the specular spike reflectance model. For specular spike surfaces, a strong reflection is observed when the angle of incidence equals the angle of reflectance. Surfaces that exhibit a specular lobe (A specular lobe exhibits a gaussian intensity profile, around its specular peak.) on top of a lambertian base follow the Torrance-Sparrow reflectance model[3]. The Torrance-Sparrow model allows surface roughness to be determined in addition to surface shape.

We seek to develop a method that can extract the surface shape and surface roughness of an object that exhibits a specular lobe. The method, which we call "four light photometric ste-

reo", uses four lights which sequentially illuminate the object under inspection, and a video camera for taking images of the object.

Conceptually, the problem we are solving has three parts: shape extraction, pixel segmentation, and roughness extraction. The shape information is produced directly by the three light and four light photometric stereo methods. After we have shape information, we can apply different techniques to determine which pixels are specular and which are nonspecular. Then, we can use the specular pixels and shape information, in conjugation with the simplified Torrance-Sparrow reflectance model to determine the surface roughness.

In section two we develop the four light photometric stereo method for different regions of a gaussian sphere. In section three, we develop a simplified version of the Torrance-Sparrow reflection model, and we develop the roughness extraction algorithm. Section four discusses various implementation issues. Results are presented in section five. In Appendix A, we review the three light photometric stereo method developed by Woodham.

1.1. Previous Work

Woodham [4] proposed the photometric stereo method to determine the surface shape of lambertian (diffuse) dominant surfaces by using three point light sources, and a reflectance map for each light source.

A number of methods have been developed to recover the shape of specular spike objects. Ikeuchi [5] used three extended sources to determine the surface orientation of specular surfaces. He determined the radiance distribution of the extended sources, and used this to predict image intensity based on surface orientation. Nayar, Weiss, Simon, and Sanderson [6] developed a system that used 127 point sources to determine the shape of specular objects. Coleman and Jain [7] proposed using four lights to detect specularities. They assumed that light source specularities were non-overlapping, and that if one light was specular, a valid surface orientation could be determined with the remaining three lights.

Healey and Binford [8] used a simplified version of the Torrance-Sparrow reflectance model to recover object curvature around the specular peak of specular lobe objects. They assumed that the surface roughness of the object was known. Nayar, Ikeuchi, and Kanade [9] developed a method for surfaces that exhibited a lambertian and specular spike component. The method used an array of extended light sources to illuminate an object from different directions. The array of extended sources guaranteed that specular reflections were detected. In addition, they were able to determine the ratio of the specular to lambertian reflection, which is related to surface roughness. Ikeuchi and Sato [10] developed a method to recover the shape and roughness of objects that follow the Torrance-Sparrow reflectance model. They took a range image using a range finder, and an intensity image using a CCD camera, using the range image to determine surface shape. Then, they used an iterative segmentation algorithm to classify pixels in the intensity image as specular or lambertian, and to determine the light source direction. Surface roughness was determined by fitting specular intensity values to a simplified version of the Torrance-Sparrow reflectance model. The use of a range finder to determine surface orientation requires taking first derivatives of the range data. This makes the method sensitive to noise.

2. Determining Surface Shape and Pixel Segmentation using Four Light Photometric Stereo

An object illuminated by four light sources will produce three categories of regions based upon illumination: regions illuminated by all four light sources, regions illuminated by three light sources, and regions illuminated by only two light sources. If we illuminate an object with four equally spaced light sources, the region map, represented on the gaussian sphere, will look like this:

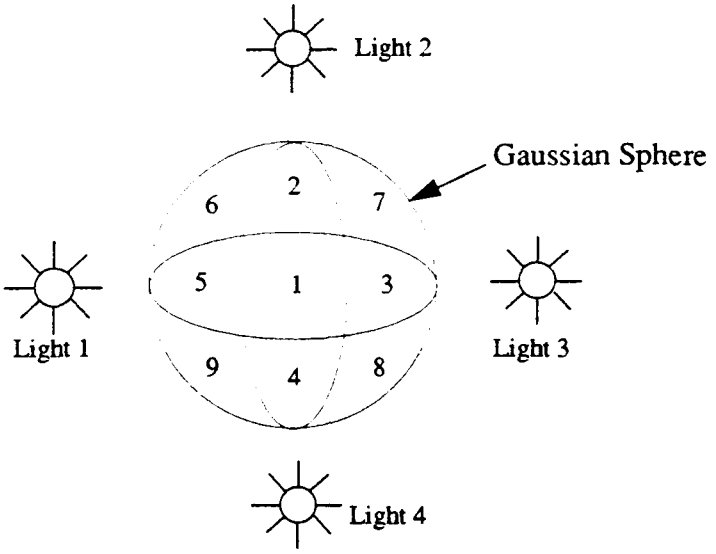

Region 1 is illuminated by all four light sources. Regions 2, 3, 4, and 5 are illuminated by three light sources. Regions 6, 7, 8, and 9 are illuminated by two light sources. The region boundaries are formed by the shadow lines of each light source. The size and shape of each region is dependent on the inclination of the light sources.

Different information is available in each of the three categories of regions. Therefore, we use different techniques for determining surface shape and for performing pixel segmentation in each region.

2.1. Determining Surface Shape and Pixel Segmentation in the Four Light Illuminated Region

Coleman and Jain proposed using four lights to determine the shape of surfaces that were nonlambertian. The method is only valid in regions illuminated by all four light sources, the region labeled 1. They proposed to calculate four albedo values based on the four possible combinations of three light sources. For a perfectly lambertian surface, the four albedos would be identical. But, for surfaces that exhibit some specularity, this is not the case. If we assume that the specular lobes of each light source do not intersect, then a specularity in one light source will cause the three albedos that use that light source to be high, while the albedo that does not use the light source will be low. Given four intensity values, (I1, I2, I3, I4), and four light source directions, (**S1, S2, S3, S4**), we can define four albedos, (Ra, Rb, Rc,

Rd), as follows:

$$\mathbf{Sa} = \begin{bmatrix} S1x & S1y & S1z \\ S2x & S2y & S2z \\ S3x & S3y & S3z \end{bmatrix} \quad \mathbf{Sb} = \begin{bmatrix} S2x & S2y & S2z \\ S3x & S3y & S3z \\ S4x & S4y & S4z \end{bmatrix} \quad \mathbf{Sc} = \begin{bmatrix} S3x & S3y & S3z \\ S4x & S4y & S4z \\ S1x & S1y & S1z \end{bmatrix} \quad \mathbf{Sd} = \begin{bmatrix} S4x & S4y & S4z \\ S1x & S1y & S1z \\ S2x & S2y & S2z \end{bmatrix}$$

$$\mathbf{Ia} = \begin{bmatrix} I1 \\ I2 \\ I3 \end{bmatrix} \quad \mathbf{Ib} = \begin{bmatrix} I2 \\ I3 \\ I4 \end{bmatrix} \quad \mathbf{Ic} = \begin{bmatrix} I3 \\ I4 \\ I1 \end{bmatrix} \quad \mathbf{Id} = \begin{bmatrix} I4 \\ I1 \\ I2 \end{bmatrix}$$

$$Ra = \left| (\mathbf{Sa})^{-1}\mathbf{Ia} \right|$$

$$Rb = \left| (\mathbf{Sb})^{-1}\mathbf{Ib} \right|$$

$$Rc = \left| (\mathbf{Sc})^{-1}\mathbf{Ic} \right|$$

$$Rd = \left| (\mathbf{Sd})^{-1}\mathbf{Id} \right|$$

(S1x, S1y, and S1z are the x, y, and z components of the unit vector to light source number one)

If I1 is specular, Ra, Rc, and Rd will be elevated above their lambertian levels. Rb will be the lambertian albedo, since I2, I3, and I4 are not specular (Our assumption is that for each image point, at most one light source will be specular.).

Therefore, we can identify the nonspecular light sources, by using the four albedos, and we can use these nonspecular light sources to produce a valid surface normal. In the above example, we would determine that Rb is the minimum albedo, and then use I2, I3, and I4 to determine the surface normal. Since the surface is lambertian, the surface normal is equal (see Appendix A) to:

$$\begin{bmatrix} S2x & S2y & S2z \\ S3x & S3y & S3z \\ S4x & S4y & S4z \end{bmatrix}^{-1} \begin{bmatrix} I2 \\ I3 \\ I4 \end{bmatrix} = \begin{bmatrix} Nx \\ Ny \\ Nz \end{bmatrix}$$

However, due to image noise, the four albedos will never be exactly equal. We need to establish a threshold to determine when the differences in albedo indicate a specularity, and when they are just due to random events. Coleman and Jain define albedo deviation, Rdev:

$$Rdev = \left(\sum_{i=a,b,c,d} (Ri - Rmean) \right) / (4Rmin)$$

If Rdev > Rt, they classify the pixel as specular, otherwise it is lambertian. Rt is a manually selected threshold. The use of an arbitrarily selected threshold makes this classification scheme ad hoc.

We propose a better classification scheme which would use the variance of the camera's intensity response to determine a statistically meaningful threshold. If σ_i^2 is the camera's intensity variance measured at a particular pixel, then we can establish a specular threshold

based on a +/-3σ distribution [11]. We assume that the light source directions are known without any uncertainty. Then, in the case where R1 is the maximum albedo and R2 is the minimum albedo, we can define Rdev as:

$$Rdev = R1 - R2$$

If Rdev is greater than the specular threshold, one of the light sources is specular.

We can determine an accurate surface normal if a pixel is specular, by using the light sources from the minimum albedo to determine the surface normal. If a pixel is not specular, we can use any of the three light sources to determine the surface normal.

2.1.1. Specular Threshold in Four Light Illuminated Region

A pixel is specular if Rdev is greater than the specular threshold:

$$Rdev > 6\sqrt{(\frac{\partial}{\partial I1}R1 + \frac{\partial}{\partial I1}R2)^2\sigma_i^2 + (\frac{\partial}{\partial I2}R1 + \frac{\partial}{\partial I2}R2)^2\sigma_i^2 + (\frac{\partial}{\partial I3}R1 + \frac{\partial}{\partial I3}R2)^2\sigma_i^2 + (\frac{\partial}{\partial I4}R1 + \frac{\partial}{\partial I4}R2)^2\sigma_i^2}$$

If an albedo does not use a particular light source, the terms involving its partial derivatives simply go to zero. The partial derivatives are not complex, and exact expressions can easily be derived. This threshold assumes a worst case 6σ separation between R1 and R2. In practice each pixel in the image has its own light intensity variance, due to variations in manufacture of the camera's CCD array. Therefore, the variance needs to be measured for each pixel.

2.2. Determining Surface Shape and Pixel Segmentation in the Three Light Illuminated Region

The region labeled 3 is illuminated by light sources 2, 3, and 4. Its borders are formed by the shadow lines of light sources 1, 4, and 2. If we assume that the specular regions of each light source are nonoverlapping, and if the surface is specular, region 3 may have a specularity from light source 3. Illumination by light sources 2 and 4 will be nonspecular in region 3.

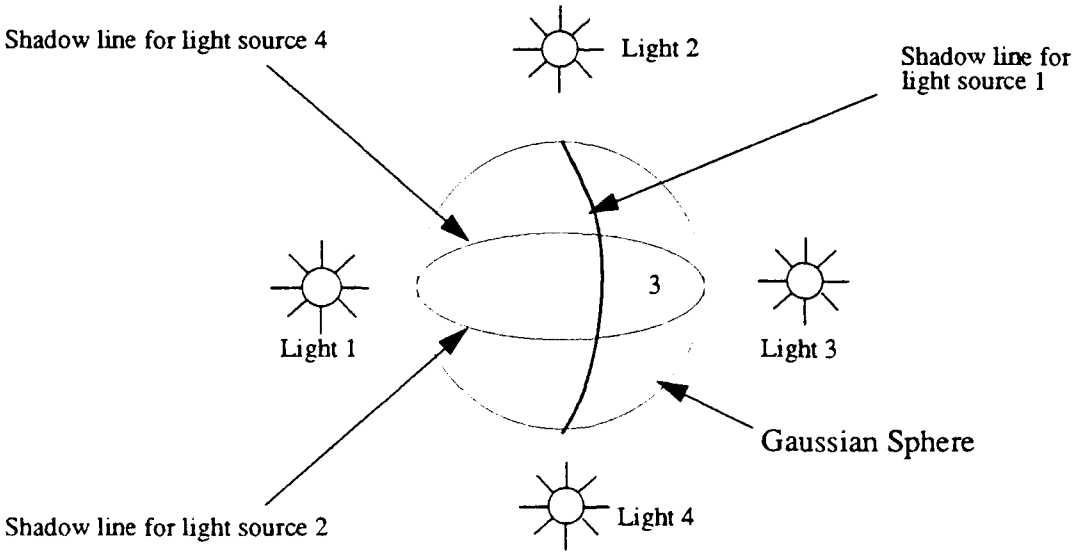

Under these assumptions, we can determine an accurate surface normal using light source 2, light source 4, and the shadow line of light source 1. We do not use light source 3 because it may be specular. We can write three equations, in three unknowns:

$$\frac{I_2}{\rho} = S2xNx + S2yNy + S2zNz$$

$$\frac{I_4}{\rho} = S4xNx + S4yNy + S4zNz$$

$$(Nx)^2 + (Ny)^2 + (Nz)^2 = 1$$

The albedo, ρ, the light source directions **S2** and **S4**, and the image intensities I2 and I4 are known. The albedo is calculated form the albedos of the lambertian pixels within a 10X10 pixel area within the four light illuminated region. The surface normal is by definition a unit vector.

This set of three equations has two sets of solutions. If we define the following intermediate variables:

$$a = \frac{S2x}{S2z} \quad b = \frac{S2y}{S2z} \quad g = \frac{I2}{\rho S2z} \qquad c = \frac{S4x}{S4z} \quad d = \frac{S4y}{S4z} \quad h = \frac{I4}{\rho S4z}$$

$$e = \frac{-g+h}{c-a} \qquad f = \frac{d-b}{c-a}$$

$$A = f^2a^2 + f^2 - 2abf + b^2 + 1$$

$$B = 2agf - 2efa^2 - 2ef + 2abe - 2bg$$

$$C = -2age + a^2e^2 + e^2 + g^2 - 1$$

The two sets of surface normal solutions are:

$$Ny_1 = \frac{-B + \sqrt{B^2 - 4AC}}{2A} \qquad Ny_2 = \frac{-B - \sqrt{B^2 - 4AC}}{2A}$$

$$Nx_1 = e - fNy_1 \qquad Nx_2 = e - fNy_2$$

$$Nz_1 = g - aNx_1 - bNy_1 \qquad Nz_2 = g - aNx_2 - bNy_2$$

The proper solution can be selected by using the boundary condition of light source one's shadow line. (It is possible that due to degenerate positioning of light sources 1, 2, and 4, that both surface normals are on the same side of light source one's shadow line. We do not consider this case.) On the shadow line of light source one, the following equation holds:

$$S1xNx + S1yNy + S1zNz = 0$$

In region number 3,

$$S1xNx + S1yNy + S1zNz < 0$$

So we can select the proper solution by seeing if this condition holds for each solution.

2.2.1. Threshold for Selecting Proper Surface Normal Solution

Selecting the proper solution becomes more complex in the presence of intensity noise, which causes uncertainty in the normals, and uncertainty in the location of the shadow line. We assume that the light source directions are known without any uncertainty. The intensity values and the albedo have variances (The albedo variance is calculated from the albedos of the lambertian pixels within a 10X10 pixel area within the four light illuminated region.). Based on these variances, we can express the uncertainty of the surface normals. (The partial derivatives of these expressions are very complex. Therefore, the partial derivatives are approximated with a discrete partial derivative.) We will continue using the example above. The light source variances are σ^2_{I2} and σ^2_{I4}. The albedo variance is σ^2_ρ. The uncertainty of the surface normals is:

$$\sigma^2_{Nx_1} = \left(\frac{\partial}{\partial I2} Nx_1\right)^2 \sigma^2_{I2} + \left(\frac{\partial}{\partial I4} Nx_1\right)^2 \sigma^2_{I4} + \left(\frac{\partial}{\partial \rho} Nx_1\right)^2 \sigma^2_\rho$$

$$\sigma^2_{Ny_1} = \left(\frac{\partial}{\partial I2} Ny_1\right)^2 \sigma^2_{I2} + \left(\frac{\partial}{\partial I4} Ny_1\right)^2 \sigma^2_{I4} + \left(\frac{\partial}{\partial \rho} Ny_1\right)^2 \sigma^2_\rho$$

$$\sigma^2_{Nz_1} = \left(\frac{\partial}{\partial I2} Nz_1\right)^2 \sigma^2_{I2} + \left(\frac{\partial}{\partial I4} Nz_1\right)^2 \sigma^2_{I4} + \left(\frac{\partial}{\partial \rho} Nz_1\right)^2 \sigma^2_\rho$$

A similar set of expressions can be derived for the variances of the second set of surface normals. Using this set of variances we can decide whether a pixel is on the correct side of the shadow line. For a pixel to confidently be in region number 3, the following relation must hold for its surface normal:

$$S1xNx_1 + S1yNy_1 + S1zNz_1 < 3\sqrt{\sigma^2_{Nx_1}(S1x)^2 + \sigma^2_{Ny_1}(S1y)^2 + \sigma^2_{Nz_1}(S1z)^2}$$

This expression expresses with a 3σ confidence that the surface normal solution is in the three light illuminated region, region number 3. We will have a similar expression for Nx_2, Ny_2, Nz_2. It is possible that we cannot confidently say that either set of surface normals is in region number 3. (This expression is false for both sets of surface normals.) These pixels are flagged with a special classification.

At this point, we have derived how to confidently determine surface normals for the three light illuminated region. We also need to classify pixels as specular or lambertian.

2.2.2. Specular classification of Pixels in the Three Light Illuminated Region

In order to classify a pixel as specular, we can determine whether its measured brightness, with respect to a given light source, is larger than its predicted lambertian brightness for the same light source. We can determine the predicted lambertian brightness of a pixel in the three light illuminated region by using the surface normal derived in the preceding section, the source directions (which are known), and the lambertian albedo. Using the example of the preceding section, we want to determine if the measured brightness due to light source three is greater than its lambertian brightness. If the derived normal vector for the pixel under consideration is (Nx, Ny, Nz), and the measured brightness of the pixel due to light source three is I3, then the pixel is specular if:

$$I3 > \rho\,(S3xNx + S3yNy + S3zNz)$$

2.2.2.1. Specular Threshold in the Three Light Illuminated Region

We need to consider the uncertainty of I3, ρ, Nx, Ny, and Nz. The uncertainty of the predicted lambertian brightness, Ilam, is σ^2_{Ilam}.

$$Ilam = \rho\,(S3xNx + S3yNy + S3zNz)$$

$$\sigma^2_{Ilam} = \left(\frac{\partial}{\partial\rho}Ilam\right)^2\sigma^2_\rho + \left(\frac{\partial}{\partial Nx}Ilam\right)^2\sigma^2_{Nx} + \left(\frac{\partial}{\partial Ny}Ilam\right)^2\sigma^2_{Ny} + \left(\frac{\partial}{\partial Nz}Ilam\right)^2\sigma^2_{Nz}$$

If σ^2_{I3} is the uncertainty of the measured brightness, then we can say that the pixel is specular, assuming a 3σ distribution, if:

$$I3 - Ilam > 6\sqrt{\sigma^2_{Ilam} + \sigma^2_{I3}}$$

2.3. Determining Surface Shape and Pixel Segmentation in the Two Light Illuminated Region

It is possible to determine the surface normal in the region illuminated by only two lights. The region labeled 7 is illuminated by light sources 2 and 3. Its borders are formed by the shadow lines of light sources 1 and 4.

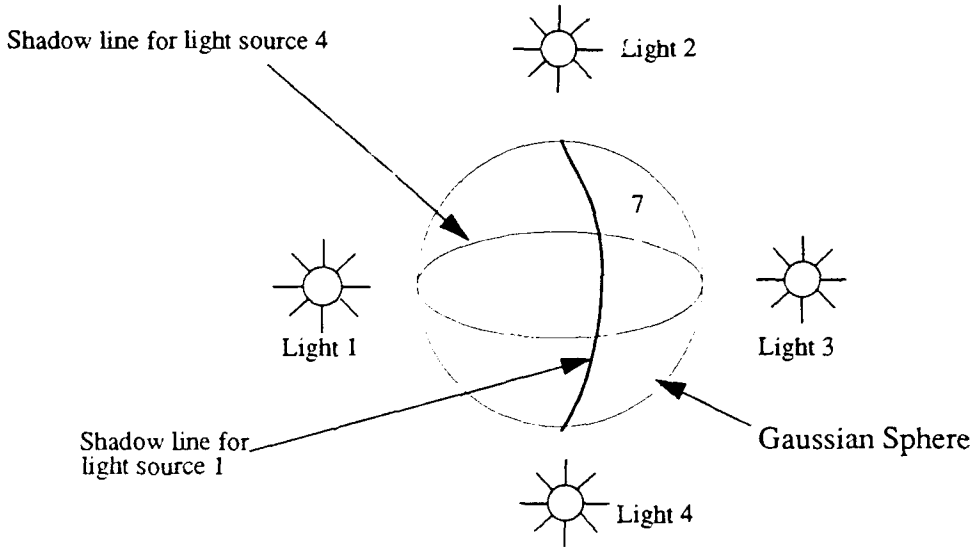

If we assume that neither light 2 nor light 3 have a specularity in region 7, we can write the

following set of equations:

$$\frac{I_2}{\rho} = S2xNx + S2yNy + S2zNz$$

$$\frac{I_3}{\rho} = S3xNx + S3yNy + S3zNz$$

$$(Nx)^2 + (Ny)^2 + (Nz)^2 = 1$$

The equations will yield two sets of surface normal solutions, and can be solved using the methods of the three light illuminated region.

The proper solution can be selected by using the boundary condition for light source one's shadow line, and the boundary condition for light source four's shadow line. In region number 7,

$$S1xNx + S1yNy + S1zNz < 0 \wedge S4xNx + S4yNy + S4zNz < 0$$

2.3.1. Threshold for Selecting Proper Surface Normal Solution

If we consider the uncertainty due to intensity noise, the following two relations must hold:

$$S1xNx_1 + S1yNy_1 + S1zNz_1 < 3\sqrt{\sigma^2_{Nx_1}(S1x)^2 + \sigma^2_{Ny_1}(S1y)^2 + \sigma^2_{Nz_1}(S1z)^2}$$

$$S4xNx_1 + S4yNy_1 + S4zNz_1 < 3\sqrt{\sigma^2_{Nx_1}(S4x)^2 + \sigma^2_{Ny_1}(S4y)^2 + \sigma^2_{Nz_1}(S4z)^2}$$

where $(Nx_1, Ny_1 Nz_1)$ is one of the surface normal solutions. A similar set of equations hold for the second set of surface normal solutions. The surface normal variances are calculated using the expressions derived for the three light illuminated region.

2.3.2. Specular Classification of Pixels in the Two Light Illuminated Region

The assumption that light source one and four do not produce a specularity in the two light illuminated region is not strong. However, if one of the lights does produce a specularity, the surface normal solutions may become imaginary. If the lambertian albedo is correct, and there are no interreflections, then the existence of imaginary surface normal solutions indicates a specularity in one of the two light sources. Pixels may not be sufficiently specular to cause the surface normal solutions to become imaginary. In this case, the surface normal solutions will be erroneous, and it will be not be possible to detect the condition.

3. Extracting Specular Intensity and Surface Roughness

The Torrance-Sparrow reflectance model allows us to determine the specular intensity and surface roughness of an object. In this section, we develop a simplified version of the Torrance-Sparrow model. Then, we develop the specular intensity and surface roughness extraction algorithms.

3.1. Simplified Torrance-Sparrow Model

The Torrance-Sparrow model is a geometrical optics model of reflection for rough surfaces. The model describes reflection for surfaces that exhibit a specular lobe.

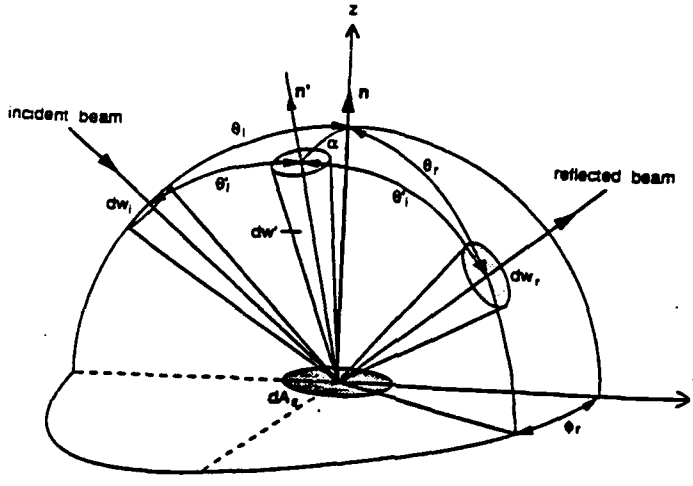

Geometry for Torrance-Sparrow Model

For a fixed incident light angle (which we assume because the light is far from the object, making the light rays parallel over the object's surface), and for a given material, the surface radiance is:

$$E = F(\theta_i', \mathbf{n}') \left[\frac{G(\theta_i, \theta_r, \phi_r)}{\cos\theta_r} \right] exp(-c^2\alpha^2)$$

$F(\theta_i', \mathbf{n}')$ is the Fresnel reflectance coefficient. (θ_i' is the local angle of incidence. $\mathbf{n}'$ is the local surface orientation. θ_i is the global angle of incidence. $\mathbf{n}$ is the mean surface orientation.) For insulators, with incident angles of less than 40 degrees, the Fresnel coefficient can be

approximated by a constant.

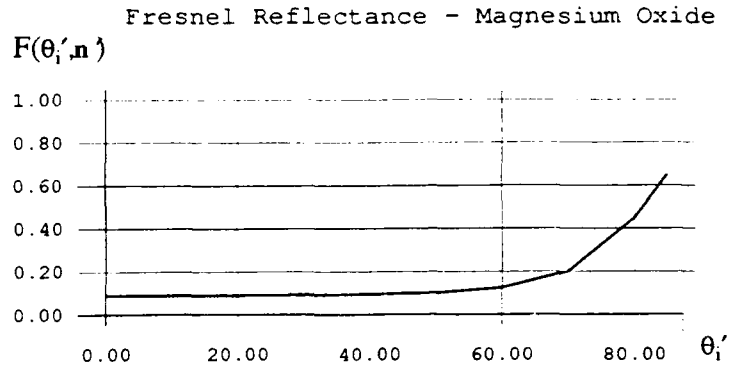

$G(\theta_i,\theta_r,\phi_p)$ is the geometric attenuation factor. This accounts for masking and shadowing of one micro facet by adjacent micro facets. For incident angles between 0 degrees and 60 degrees, and reflected angles between 0 degrees and 80 degrees, the geometric attenuation factor is close to unity.

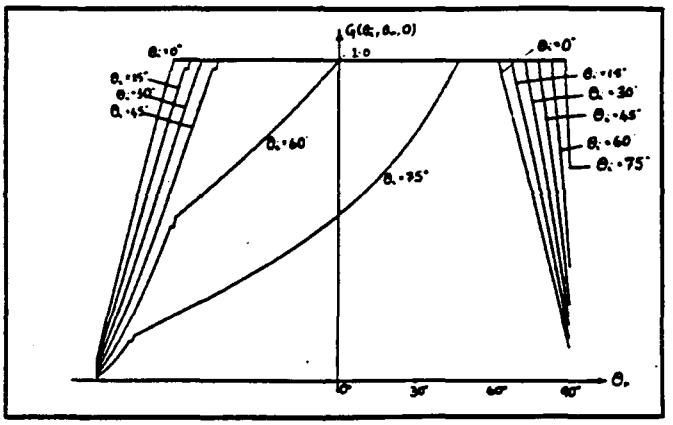

Typical Plot of Geometric Attenuation Factor

With these assumptions we can simplify the Torrance-Sparrow model to:

$$E = B\left(\frac{exp(-c^2\alpha^2)}{\cos\theta_r}\right)$$

B is a constant which we will call the specular intensity.

If the camera is at N=(0,0,1), then $\cos\theta_r$ simplifies to Nz (the z component of the surface normal). "c" is a constant that is proportional to the surface roughness. So c^2 can be replaced with "K". If we determine K, we can find out how rough a surface is. We then have:

$$E = B\left(\frac{exp(-K\alpha^2)}{Nz}\right)$$

The total surface radiance will be the sum of the underlying lambertian radiance, A, and the

radiance of the specular lobe.

$$E = A + B\left(\frac{exp(-K\alpha^2)}{Nz}\right)$$

3.2. Specular Intensity and Surface Roughness Extraction Algorithm

Once the surface shape is determined and the specular pixels are extracted, the specular intensity and surface roughness can be determined. In the simplified Torrance-Sparrow model, we need to determine B, the specular intensity, and K, the specular sharpness which is proportional to the surface roughness. We use the following algorithm:

1. Using the extracted surface normals and lambertian albedo, we can determine the lambertian intensity at each image point.
$$A = \rho(SxNx + SyNy + SzNz)$$

2. We can define D, the difference between the measured image brightness at each specular pixel and the lambertian intensity.
$$D = I - A$$

3. α can be determined from the light source direction, which is known, and from the surface normal, which is also known.

4. B and K can be determined by an iterative least square fitting. If we start out with an initial guess for B, we can estimate K.

   Our model is:
$$D = B\left(\frac{exp(-K\alpha^2)}{Nz}\right)$$

   We can linearize the model with respect to K, by taking the natural log:
$$lnD + lnNz - lnB + K\alpha^2 = 0$$

   The difference between the D and the specular part of the Torrance-Sparrow model, using our current estimate of B and K, is the error in fit between our measurements and our model:
$$lnD + lnNz - lnB + K\alpha^2 = \varepsilon_2$$

   The total error over all the specular pixels, (i,j), in the image is:
$$P = \sum_{i,j} [lnD(i,j) + lnNz(i,j) - lnB + K\alpha^2(i,j)]^2$$

   We want to find the minimum of the error with respect to K. This happens when:

$$\frac{\partial P}{\partial K} = 0 = \sum_{i,j} \alpha^2(i,j)\,(lnD(i,j)) + \sum_{i,j} \alpha^2(i,j)\,(lnNz(i,j)) - lnB\sum_{i,j} \alpha^2(i,j) + K\sum_{i,j} \alpha^4(i,j)$$

K is then simply:

$$K = \frac{-\sum_{i,j} \alpha^2(i,j)\, lnD(i,j) - \sum_{i,j} \alpha^2(i,j)\, lnNz(i,j) + lnB \sum_{i,j} \alpha^2(i,j)}{\sum_{i,j} \alpha^4(i,j)}$$

5. Using the value of K, just obtained, we can derive a value for B.

   The expression for the difference between D and the specular part of the Torrance-Sparrow model is already linear in B. We can write an expression for the error over all the specular pixels as:

$$P = \sum_{i,j} \left[D(i,j) - \frac{B exp(-K\alpha^2(i,j))}{Nz(i,j)} \right]^2$$

   Taking the partial derivative of the total error with respect to B, we obtain:

$$\frac{\partial P}{\partial B} = 0 = \sum_{i,j} \frac{(exp(-K\alpha^2(i,j))\, D(i,j))}{(Nz(i,j))} - B \sum_{i,j} \left[\frac{(exp(-K\alpha^2(i,j)))}{(Nz(i,j))} \right]^2$$

   Therefore B is:

$$B = \frac{\sum_{i,j} \frac{exp(-K\alpha^2(i,j))\, D(i,j)}{Nz(i,j)}}{\sum_{i,j} \left[\frac{(exp(-K\alpha^2(i,j)))}{(Nz(i,j))} \right]^2}$$

6. Steps 4 and 5 are repeated until the values of B and K converge.

4. Implementation

4.1. Determining Light Source Directions

The accuracy of the light source directions is very important to the determination of the surface shape and consequently to the extraction of the surface roughness. A number of techniques have been tested. The simplest technique is to use the brightest point on the surface of a lambertian sphere. The normal of the brightest point is coincident with the vector pointing to the light source. Although the method is simple to implement, it is sensitive to noise. Since the single brightest point, or a small group of the brightest points, is used to determine the source direction, image intensity noise makes their absolute magnitude uncertain.

A second method is to fit a lambertian reflectance function (a cosine) to the 100 brightest pixels. Since the data around the peak of the cosine is flat, the fit is not very stable. If the number of points (the threshold used to select the points) changes, the light source direction will change. This is not very reassuring.

This method can be significantly improved by obtaining a more stable fit. A more stable fit can be obtained by using points extending from the brightest part of the cosine, to the shadow area of the cosine. This fit will be stable. If the threshold is changed, within reasonable amounts, the light source direction will not change.

We find the light source directions by performing a least square fit on the intensity data of a lambertian sphere. The least squares formulation contains a residual term. This term allows the dark current value of the camera to be recovered. This value is subsequently subtracted from all images.

The intensity at each point on the lambertian sphere is:

$$A = \rho\,(SxNx(i,j) + SyNy(i,j) + SzNz(i,j))$$

The total error over the entire image between the measured intensity, E(i,j), and the intensity given by the lambertian model, using our solution for (Sx,Sy,Sz,D), where D is the residual, dark current term, is:

$$P = \sum_{i,j} [E(i,j) - SxNx(i,j) - SyNy(i,j) - SzNz(i,j) - D]^2$$

We want to find the minimum of the error with respect to (Sx,Sy,Sz,D). This happens when:

$$\frac{\partial P}{\partial Sx} = 0 = \sum_{i,j} Nx(i,j)\,(E(i,j) - SxNx(i,j) - SyNy(i,j) - SzNz(i,j) - D)$$

$$\frac{\partial P}{\partial Sy} = 0 = \sum_{i,j} Ny(i,j)\,(E(i,j) - SxNx(i,j) - SyNy(i,j) - SzNz(i,j) - D)$$

$$\frac{\partial P}{\partial Sz} = 0 = \sum_{i,j} Nz(i,j)\,(E(i,j) - SxNx(i,j) - SyNy(i,j) - SzNz(i,j) - D)$$

$$\frac{\partial P}{\partial D} = 0 = \sum_{i,j} E(i,j) - SxNx(i,j) - SyNy(i,j) - SzNz(i,j) - D$$

This set of four equations can be solved directly for Sx, Sy, Sz, and D.

4.2. Image Intensity Normalization

Normalization of the four image intensities, to compensate for differences in illumination strength, is critical to extracting surface shape, and subsequently to the extraction of surface roughness. The most common technique uses the brightest pixel in the image as a normalizing factor, and is susceptible to image intensity noise inaccuracies. Using a larger number of points is makes this technique more robust.

In order to normalize the light sources, each light source needs to illuminate points that have the same camera/surface normal/light source geometry. Theoretically these points will have the same brightness. An arbitrary object is not guaranteed to have such a set of points. Our solution is to use the lambertian sphere. The sphere exposes the same set of surface normals to all light sources.

After we have solved for the light source's direction, we can fit a cosine to a plot of intensity versus incident angle. The magnitude of the cosine is our normalization factor.

Below is a image of a lambertian sphere, a plot of intensity versus incident angle (using the extracted light source direction) and a best fit cosine (magnitude = 143).

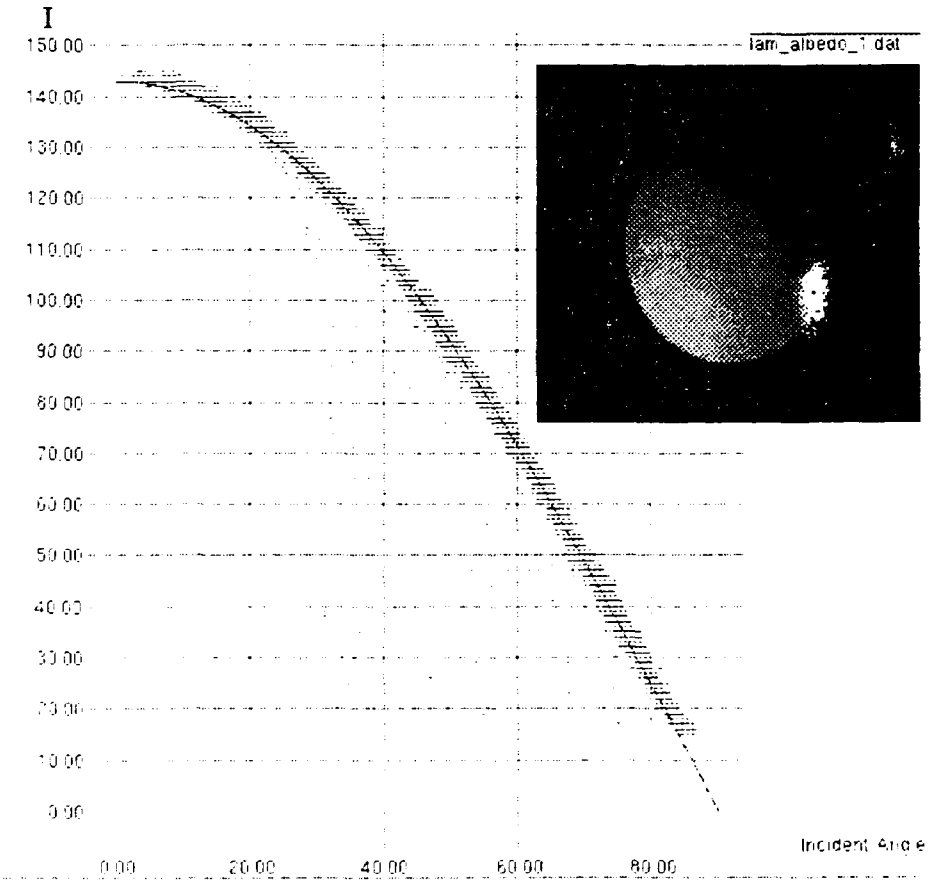

4.3. Image Linearization

Based on the known optical densities of the CMU Color Chart, and the calculated illumination strength, expected intensities from our CCD camera can be computed. An image is taken of the calibration chart. The measured and computed intensities are compared, and a table of correction factors is generated. Then, images taken with the camera can be linearized by using the table.

4.4. Image Intensity Variance

The image intensity variance, σ^2_i, was determined by taking 100 intensity images of a fixed scene, with the CCD camera. The intensity variance was then computed, for each pixel, from the 100 intensity values.

4.5. Imaginary Surface Normal Solutions in Three Light Region

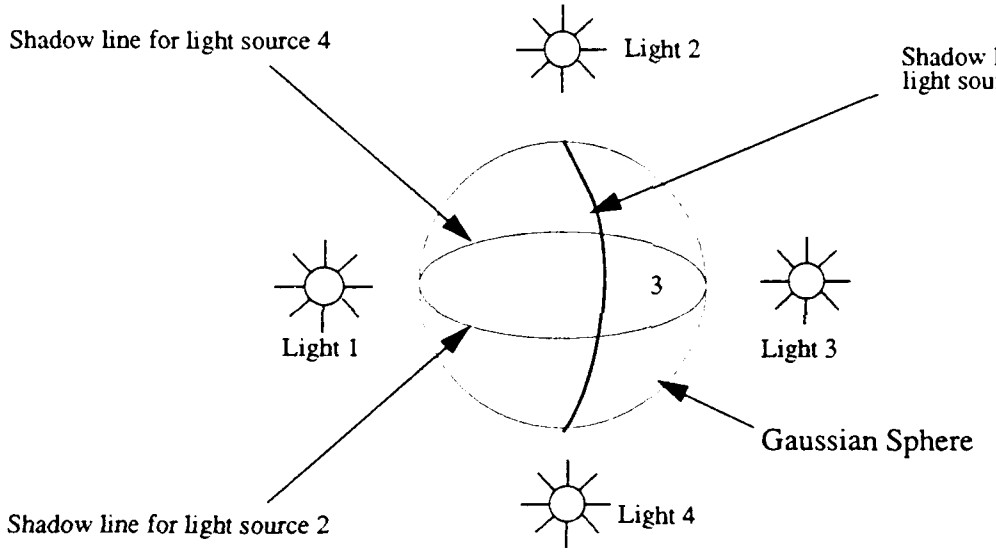

It is possible that the surface normal solutions in the three light illuminated region will be imaginary. This can happen when one pixel is brighter than a lambertian pixel could be, as interreflection or an unexpected specularity, would cause. It can also occur if there is an error in the lambertian albedo, ρ. The existence of an imaginary solution can be understood with the following description. The solution to the set of equations corresponds to finding the points on a lambertian gaussian sphere that are the intersections of two isobright contours. One isobright contour is caused by S2, and has intensity I2. The other isobright contour is produced by S4, and has intensity I4. If we imagine that we are illuminating a gaussian sphere (which contains all surface normals), these two isobright contours will be two circles. The two circles will in general intersect in at most two places. These two intersection points correspond to the two real solutions to the surface normal equations. However, if one circle gets smaller (which corresponds to the pixel getting brighter, as might be caused by interreflection), at some point the isobright contours will fail to intersect. When the contours fail to intersect, the solutions to the surface normal equations will become imaginary.

4.6. Consistent Segmentation

There is no guarantee that the statistical segmentation of specular and lambertian pixels within the three light illuminated region and the four light illuminated region will produce consistent segmentations. The uncertainty of the segmentation in the three light illuminated region has a higher uncertainty than the segmentation in the four light illuminated region. The derivation of the surface normals in the three light illuminated region involves a lot of computation; this increases their variance, making σ^2_{Ilam} large.

In order to produce consistent segmentations, we increase the uncertainty threshold of the four light illuminated region by 2X, to match three light illuminated region. The amount of increase was found by observing the segmentation of synthesized images.

Therefore, a pixel in the four light illuminated region is specular if:

$$Rdev > 12\sqrt{\left(\frac{\partial}{\partial I1}R1+\frac{\partial}{\partial I1}R2\right)^2\sigma_i^2+\left(\frac{\partial}{\partial I2}R1+\frac{\partial}{\partial I2}R2\right)^2\sigma_i^2+\left(\frac{\partial}{\partial I3}R1+\frac{\partial}{\partial I3}R2\right)^2\sigma_i^2+\left(\frac{\partial}{\partial I4}R1+\frac{\partial}{\partial I4}R2\right)^2\sigma_i^2}$$

4.7. Extracting Roughness and Specular Sharpness for Surfaces with a Weighted Lambertian Albedo

The Torrance-Sparrow model includes a diffuse component that follows the lambertian model, a cosine function. Some surfaces do not have a pure cosine function for the underlying lambertian albedo. They have a weighted lambertian albedo. For example:

$$I = A\cos\Theta + C(90° - \Theta)\cos\Theta + B\left(\frac{exp(-K\alpha^2)}{Nz}\right)$$

Below is a graph of the lambertian albedo with A = 100, and C = 0.1, and C = 0.0.

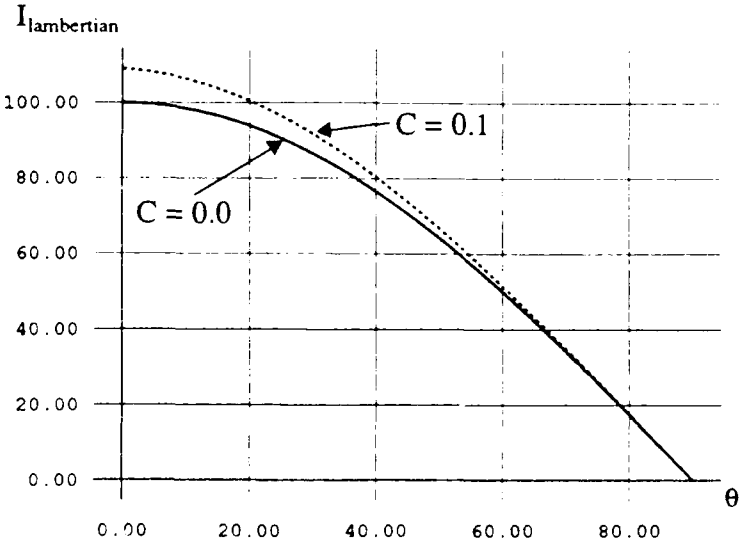

Between 50 degrees and 90 degrees, the difference between the pure cosine and the weighted cosine is small. As the angle between the surface normal and the incident light becomes smaller, the difference between the two albedos becomes larger. We have previ-

ously assumed a uniform albedo over the object's surface. This is not the case here. Extraction of the lambertian albedo (assuming that it did follow a cosine function) at different points on the object's surface will yield different results.

The lambertian albedo impacts the calculations in a number of different ways. The calculation of surface normals, in the three light and four light illuminated regions, depends on the accuracy of the lambertian albedo. First, an error in the lambertian albedo will translate into errors in the accuracy of the surface normals. Secondly, D equals the difference between the measured image brightness at each specular pixel and the lambertian intensity. The calculation of D will be erroneous if the lambertian albedo is in error. Both of these errors, will cause errors in the extraction of the specular intensity and surface roughness.

The solution to this problem will depend, to some extent, upon the specific geometry of the imaging system. Let us assume a geometry, and see how we can overcome the errors mentioned above. Our camera will be at (0,0,1). The angle between the incident light and our camera axis will be 65 degrees. The angle between the four light sources, in the X/Y plane, will be 90 degrees. (The lights are placed at the four corners of a box.)

With this geometry, the four light illuminated region extends from 40 degree incident to 90 degree incident. Within most of this region, the theoretical cosine lambertian albedo is close

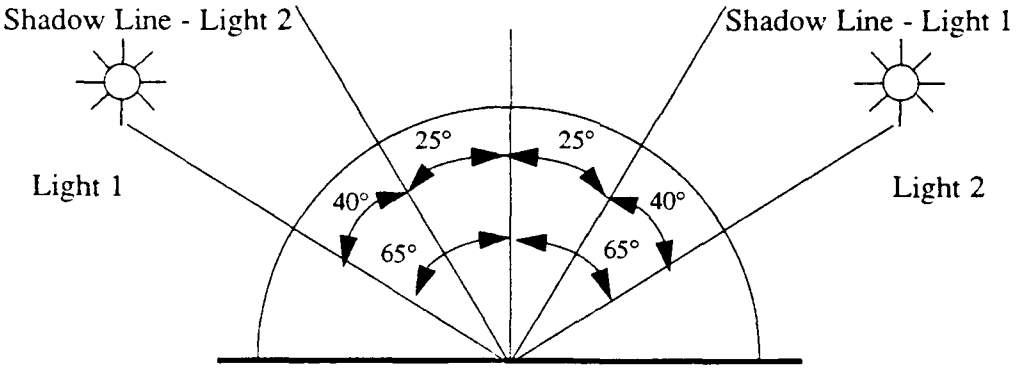

to the weighted lambertian albedo. Therefore, we can approximate the weighted lambertian albedo with a regular cosine function in this region. We can estimate the magnitude of the lambertian albedo by computing the lambertian albedo from a 100 X 100 pixel box within the four light region. So using the cosine approximation, we can extract fairly accurate surface normals, and compute a reasonable value for D, in the four light illuminated region.

The real problem exists in the three light illuminated region. In this region, we compute the

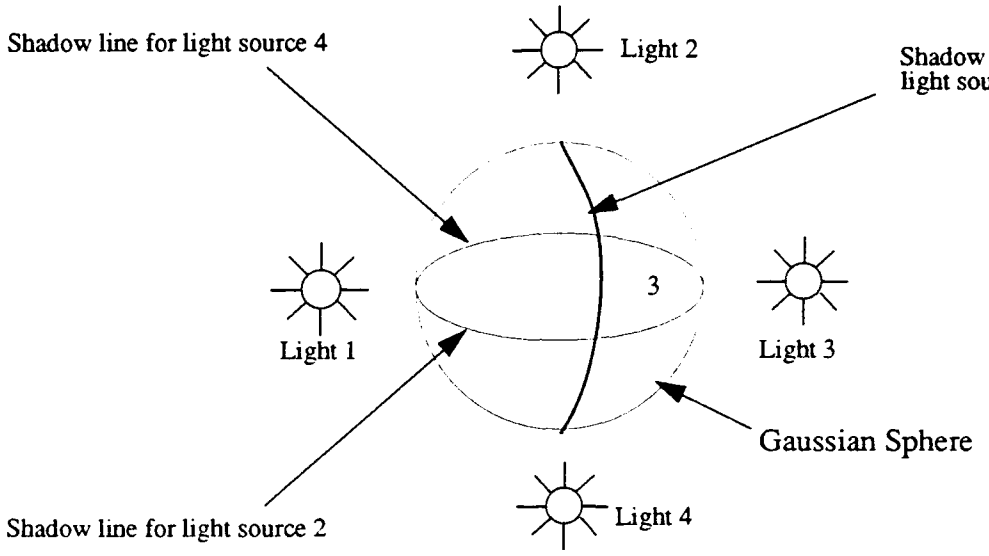

surface normals using the light sources adjacent to light source 3 (light sources 4 and 2). The angle between the adjacent light sources and the three light illuminated region will place most of the region within the 50 degree to 90 degree range. So, the surface normals computed with the unweighted lambertian albedo (from the four light illuminated region), will be fairly accurate. The value of D, computed from the light source 3, will be in error. The angle between light source 3 and the three light illuminated region will be between 0 degrees and about 40 degrees. At 0 degrees, a difference of about 10 pixel intensity levels exists between the weighted albedo and the unweighted albedo. This is a 10% error. While this error is small, it is sufficient to cause substantial errors in the specular intensity and surface roughness. The 10 pixel intensity error is only 10% of the lambertian brightness, but it is probably a much greater percentage of the specular intensity.

A specular reflection model which includes this error is needed. We modify the simplified Torrance-Sparrow model to include an offset term.:

$$D = B\left(\frac{exp(-K\alpha^2)}{Nz}\right) + Offset$$

Where the offset is the difference between the unweighted lambertian albedo and the weighted lambertian albedo. This equation has three unknowns, B, K, and the Offset. It is not possible to linearize this equation, in order to extract K. The equation can be solved by simultaneously searching for a solution in three dimensional (B,K, Offset) space.

We can define the CHISQR error as the difference between the actual value of D, the difference between the measured image brightness at each specular pixel and the lambertian intensity, and the value of D based on the current value of (B,K, Offset).

$$CHISQR = \sum_{i,j} [\,(I(i,j) - A(i,j)) - D(B,K,Offset)\,]^2$$

CHISQR is a measure of how good the current estimate of (B,K, Offset) fits the actual image data. When CHISQR equals zero the model fits the data exactly. We can search in 3D

CHISQR space for the minimum value of CHISQR. This point will give us the best estimate of (B, K, Offset).

The search direction can be determined using a variety of methods such as line search, gradient descent search, and conjugate gradient descent search. We chose gradient descent. It offers a reasonable trade-off between algorithmic complexity and search efficiency. We can define the gradient of CHISQR in each of the three dimensions, (B, K, Offset).

$$\nabla_B CHISQR = \frac{CHISQR((B, K, OFFSET) + \delta B) - CHISQR(B, K, OFFSET)}{\delta B}$$

$$\nabla_K CHISQR = \frac{CHISQR((B, K, OFFSET) + \delta K) - CHISQR(B, K, OFFSET)}{\delta K}$$

$$\nabla_{Offset} CHISQR = \frac{CHISQR((B, K, OFFSET) + \delta Offset) - CHISQR(B, K, OFFSET)}{\delta Offset}$$

The gradients are normalized with respect to the unit vector formed by the three components, (B, K, Offset). Then, the negative of the gradient is multiplied by the step size (δB, δK, δOffset) and is added to the previous value of (B, K, Offset) to produce the new search point.

The search continues until the value of CHISQR reaches a minimum.

4.8. Algorithm Flowchart

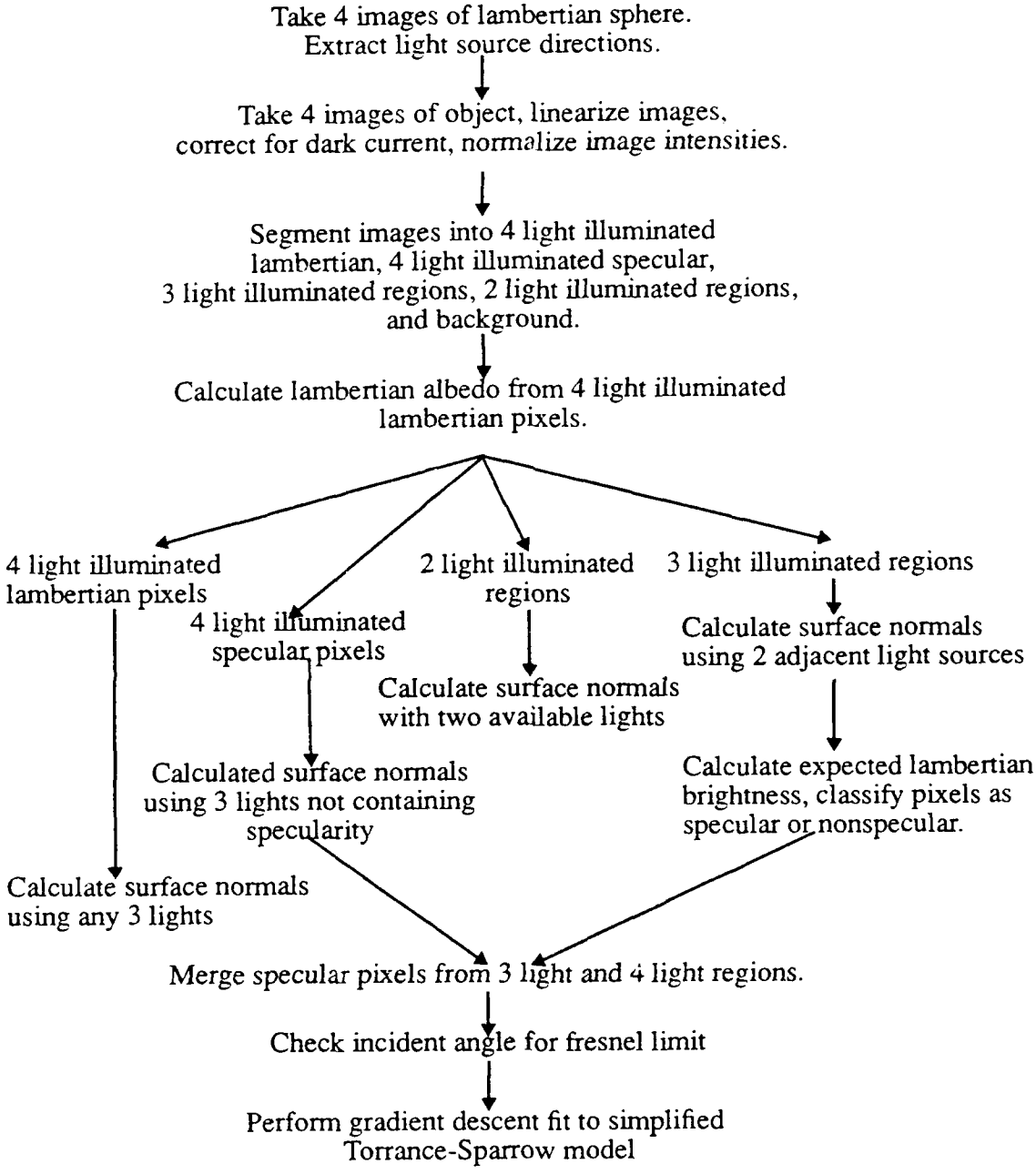

5. Results

5.1. Simulations:

Synthesized images of a sphere, including gaussian intensity noise, were created to test the validity of our algorithms.

5.1.1. Synthesized Images

Four images of a synthetic sphere were generated with the following light source directions:

	Sx	Sy	Sz
light source one	-.541	.681	.494
light source two	.661	.588	.466
light source three	.592	-.632	.499
light source four	-.631	-.555	.541

Image characteristics are: $\rho = 147$, $B = 50$ $K = 16$, $\sigma^2_i = 0.8$. (The value of $\sigma^2_i = 0.8$ is the average measured image intensity variance. Our images were reduced by a factor of four to one. Four pixels were averaged to produce one resulting pixel. The value of σ^2_i reflects this.)

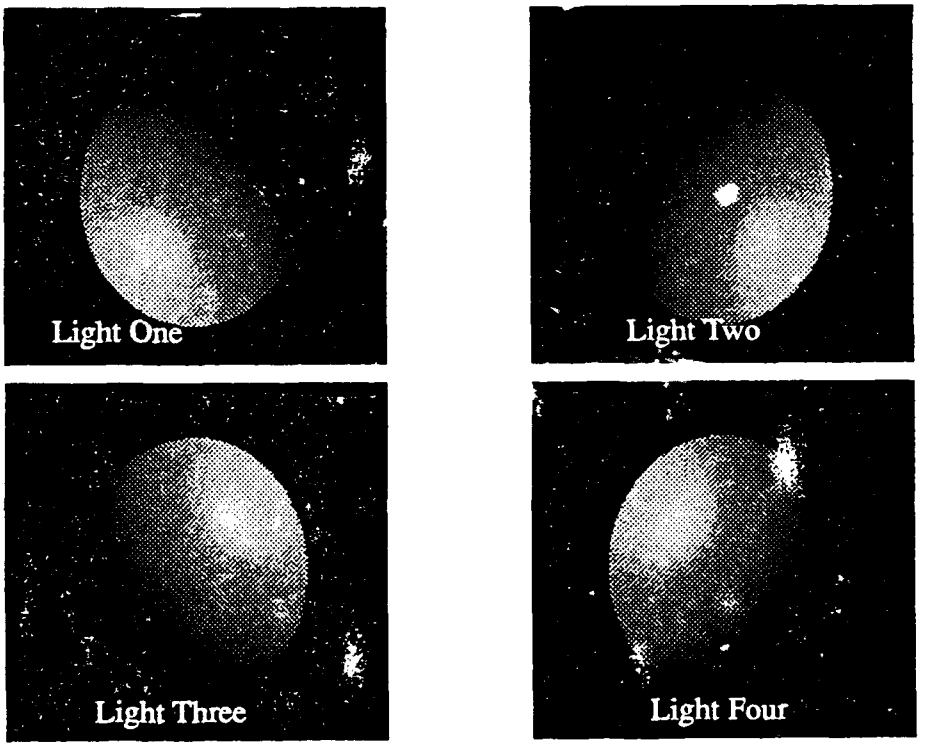

The pixel segmentation for the above images is:

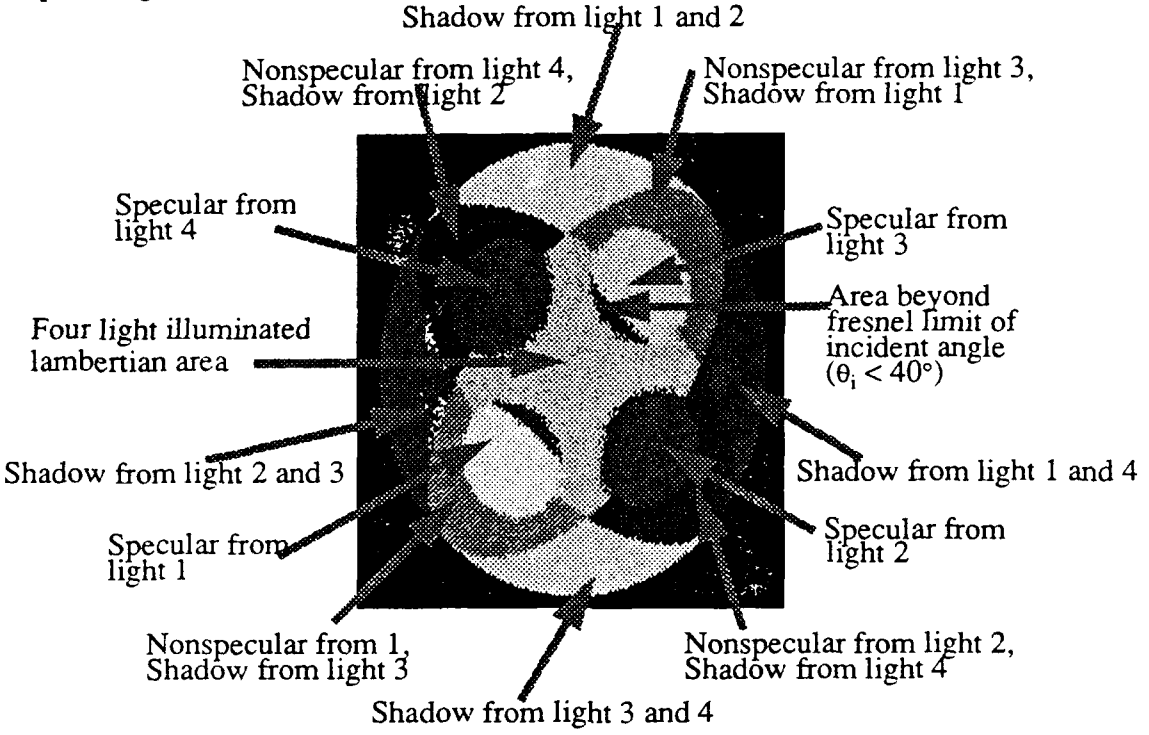

The needle map produced from the four intensity images is:

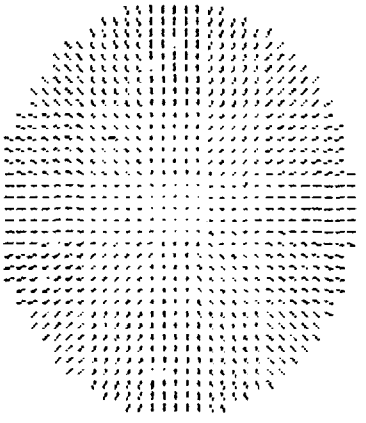

The specular intensity, B, specular sharpness, K, and the offset, Offset, extracted for the four specular spots is:

	Offset	B	K
Specular from light source one	-0.5	48.5	15.9
Specular from light source two	-3.6	51.2	14.6
Specular from light source three	-0.3	48.4	16.0
Specular from light source four	-0.5	48.3	15.9
Average values	-1.2	49.1	15.6

The plot of intensity versus incident angle for light source two is:

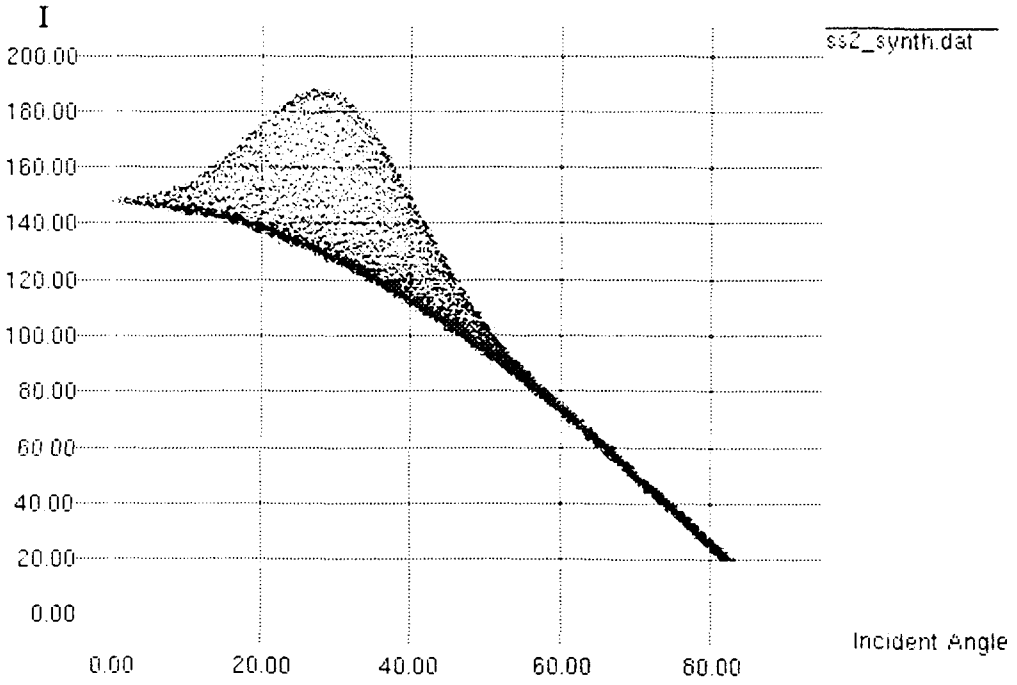

If our data follows the simplified Torrance-Sparrow model, a plot of Ln(D*Nz) versus α^2 should be linear. This can be seen from:

$$D = B\left(\frac{exp(-K\alpha^2)}{Nz}\right)$$

$$Ln(DNz) = (-K\alpha^2) + Ln(B)$$

The plot of α^2 versus ln(D*Nz) for light source two is:

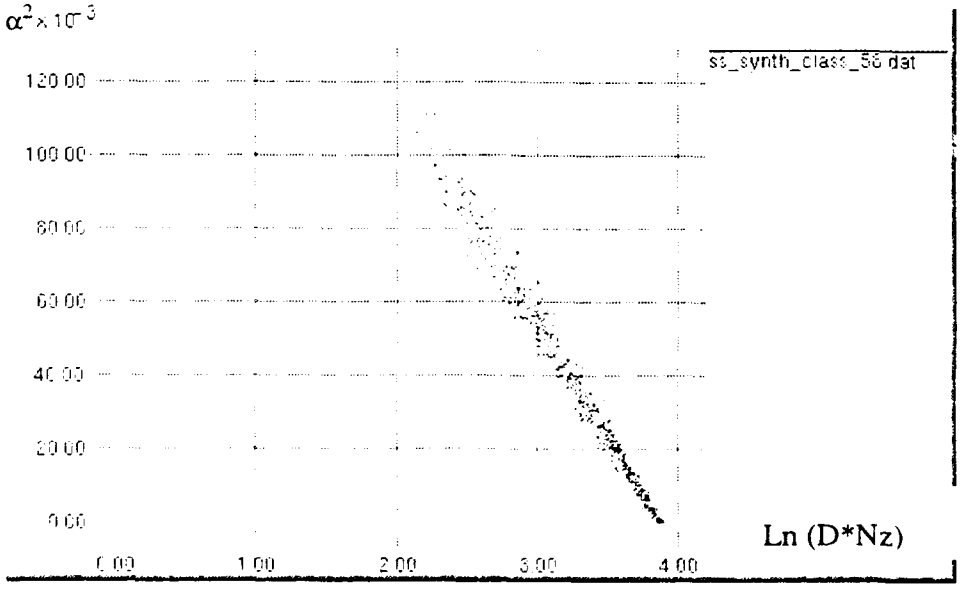

5.2. Experimental Results

The experimental results consist of images of two objects, a specular painted sphere and a plastic helmet. Both objects exhibit a specular lobe. In addition, images of a specular plastic bottle are included. The bottle exhibits a specular spike. So, it does not conform to our reflectance model assumptions, but we are able to extract the bottle's shape.

5.2.1. Experimental Setup

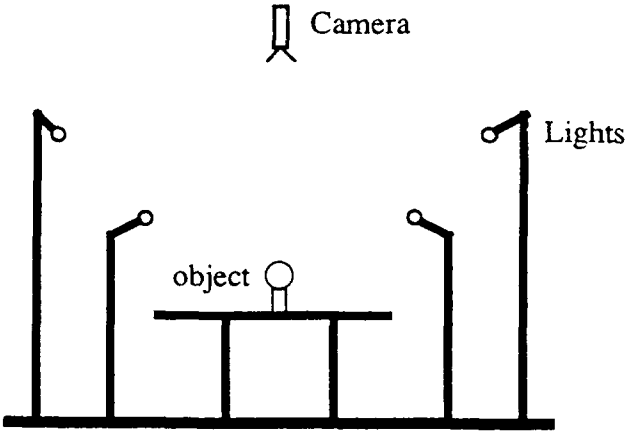

A ceiling mounted, Sony XC-57 camera, with an 85 mm Nikkor lens, was used. The camera to object distance was approximately 2.5 meters. Four ECA, 250 watt, light bulbs were mounted on light stands. The bulb to object distance was approximately 2.6 meters.

5.2.2. Painted Specular Sphere

Four images of a painted, 12.7cm diameter, sphere were taken. Light source directions were determined to be:

	Sx	Sy	Sz
light source one	-.541	.681	.494
light source two	.661	.588	.466
light source three	.592	-.632	.499
light source four	-.631	-.555	.541

Raw image data was linearized, and normalized

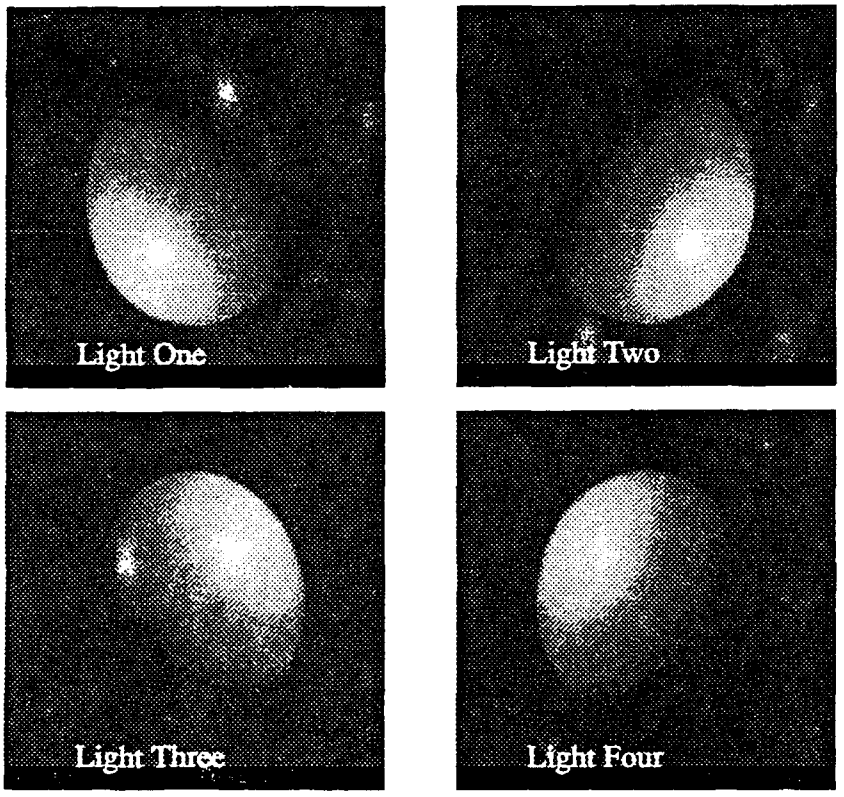

The pixel segmentation for the above images is:

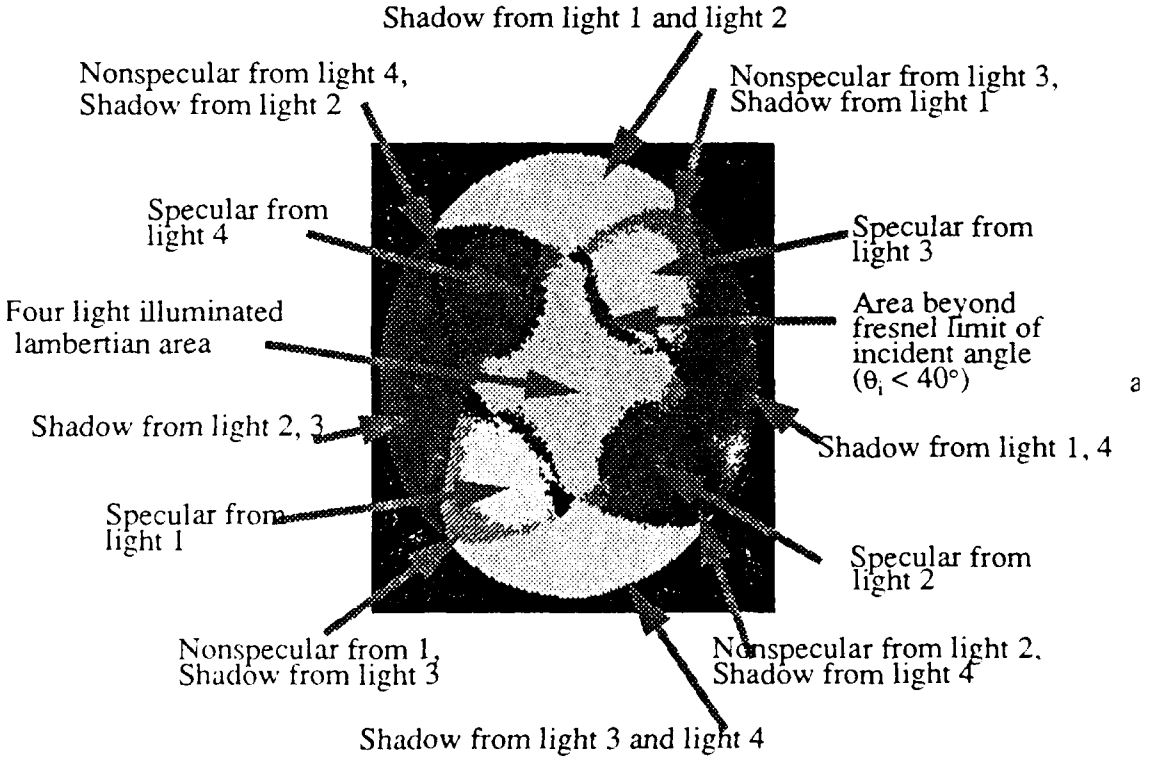

The needle map, using extracted lambertian albedo =139.8, produced from the four intensity images is:

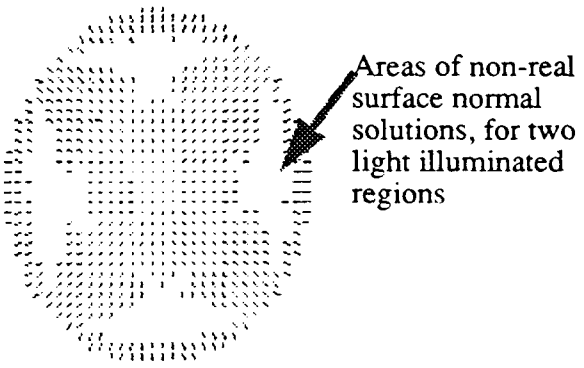

If we increase the lambertian albedo by the Offset, we are able to extract the surface normals in the two light illuminated regions.

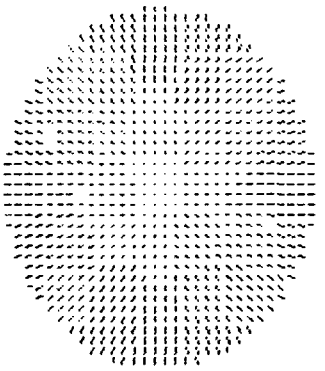

The specular intensity, B, specular sharpness, K, and the offset, Offset, extracted for the four specular spots is (The extracted lambertian albedo, ρ, is 139.8.):

	Offset	B	K
Specular from light source one	10.1	43.5	16.7
Specular from light source two	8.2	55.1	17.0
Specular from light source three	14.6	45.8	21.2
Specular from light source four	15.1	39.9	22.8
Average values	12.0	46.1	19.4

The plot of measured intensity versus incident angle for light source three is:

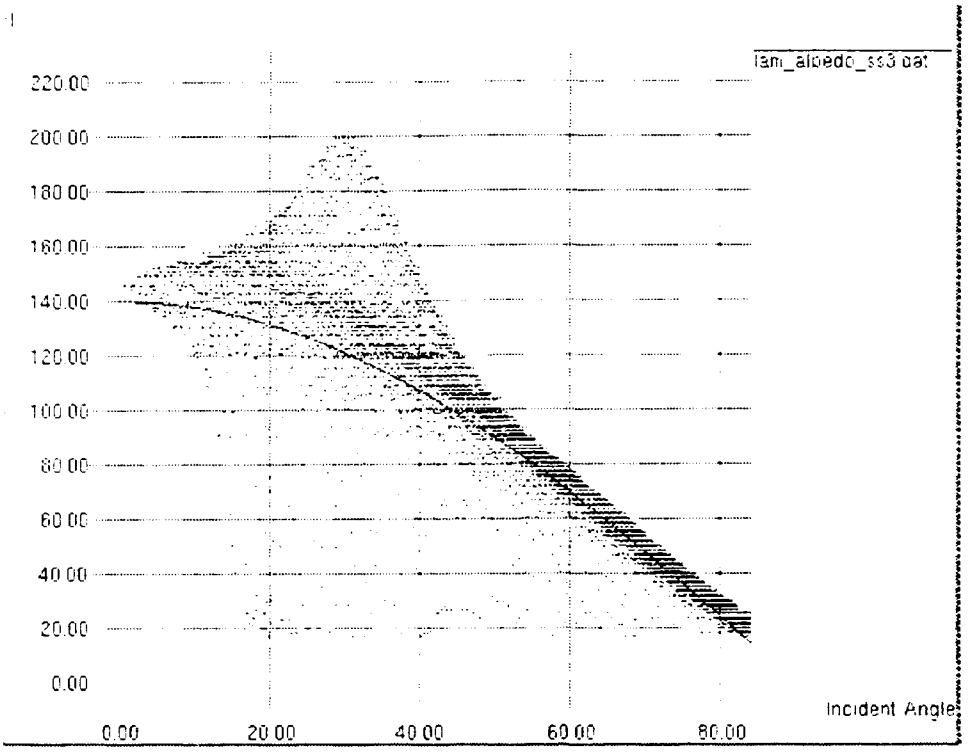

The plot of the intensity versus incident angle using the extracted values of B, K, and Offset for the specular spot due to light source three is (For this plot, since the area of interest is the specular lobe, the lambertian albedo is the sum of Offset and ρ.):

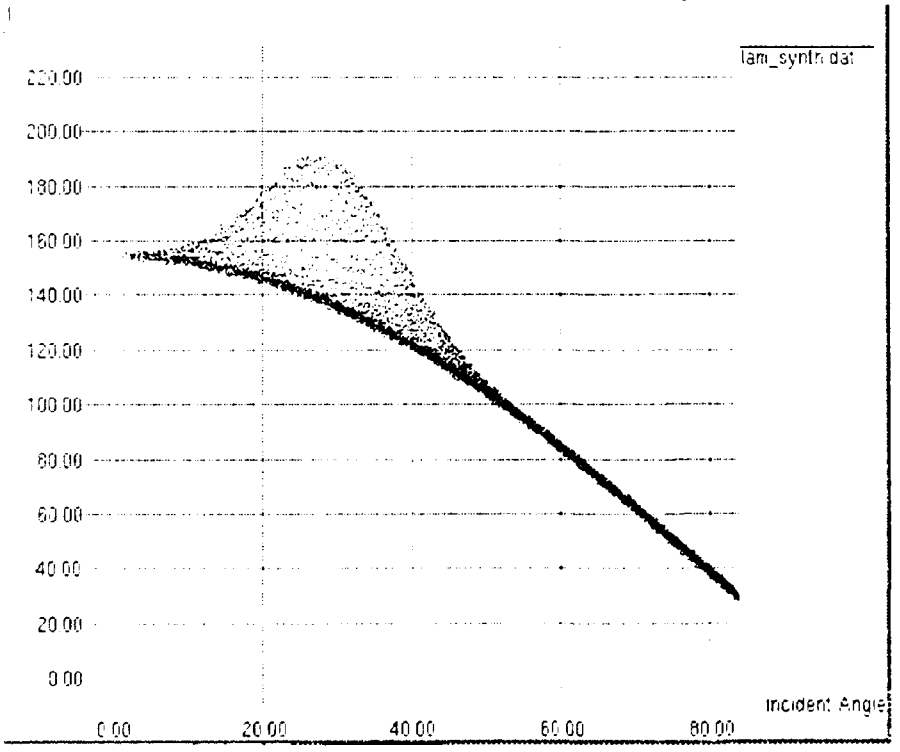

The plot of measured intensity versus incident angle for light source two is:

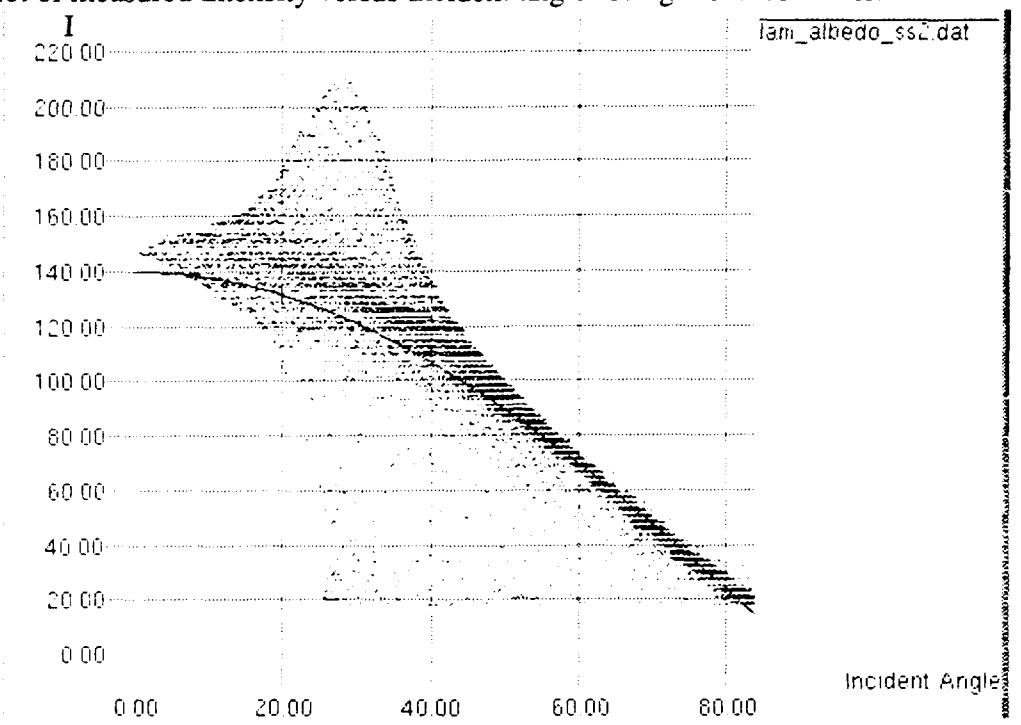

One should note the difference in magnitude between the lambertian albedo's cosine curve near the specular part of the intensity plot, and the intensity data.

The plot of the intensity versus incident angle using the extracted values of B, K, and Offset for the specular spot due to light source two is (For this plot, since the area of interest is the specular lobe, the lambertian albedo is the sum of Offset and ρ.):

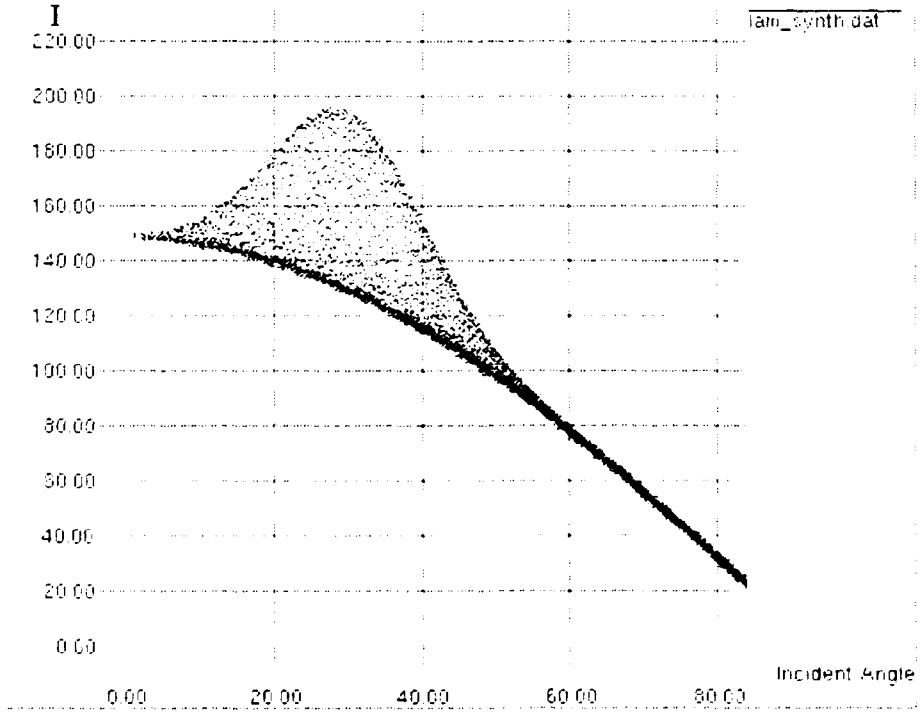

The plot of α^2 versus ln(D*Nz) is:

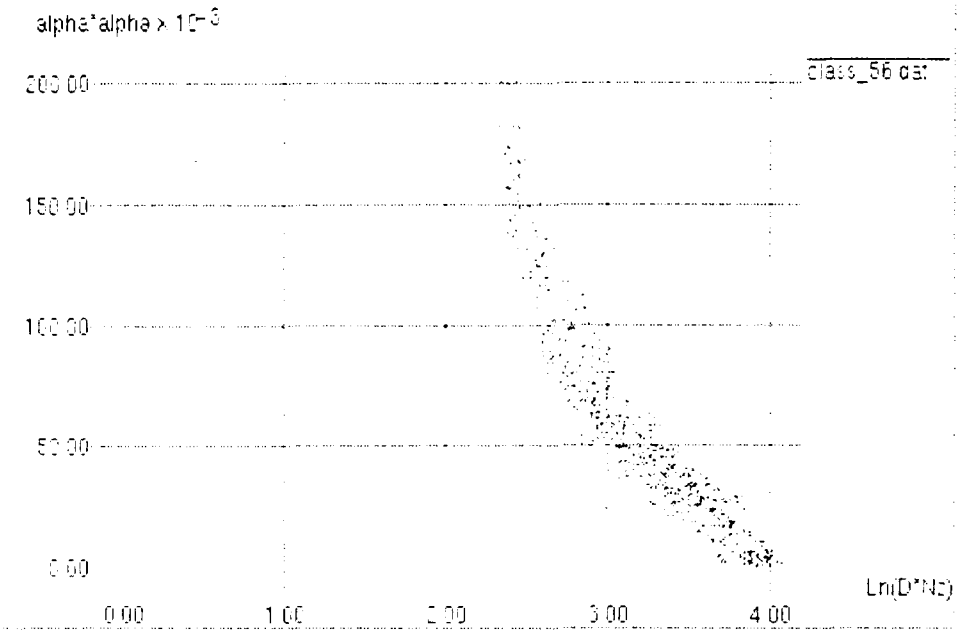

One should note the nonlinearity of the plot. This is caused by the Offset term of our model. When we compensate for the Offset, the plot becomes linear.

The plot of α^2 versus ln[(D-Offset)*Nz] is:

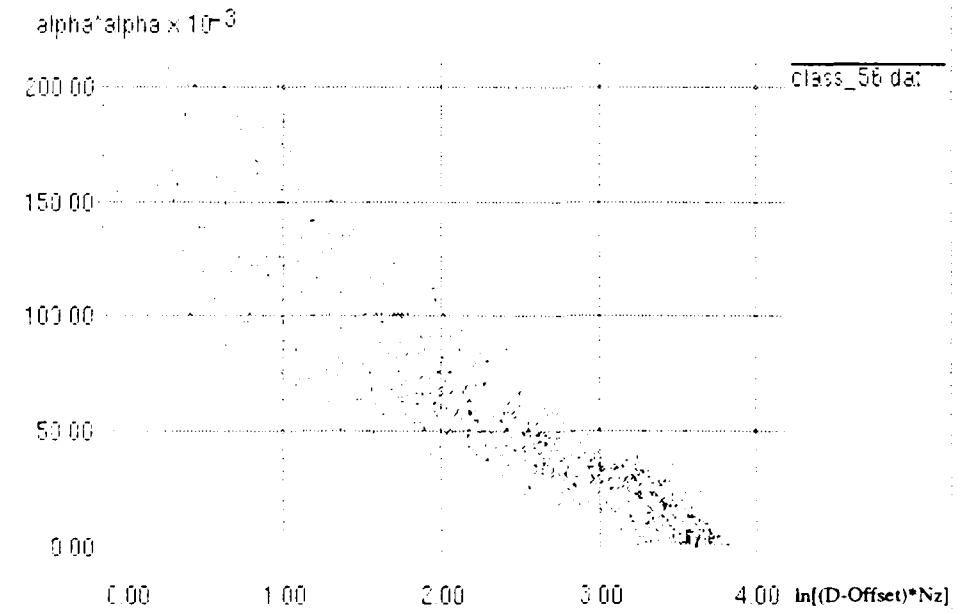

5.2.3. Plastic Helmet

Four images were taken of a plastic helmet using the following light source directions:

	Sx	Sy	Sz
light source one	-.523	.661	.539
light source two	.605	.588	.537
light source three	.601	-.587	.542
light source four	-.581	-.621	.526

The four images contain interreflections due to concavities in the surface of the helmet. Since our model does not include interreflection, we manually segmented the images to eliminated any areas where interreflection might occur.

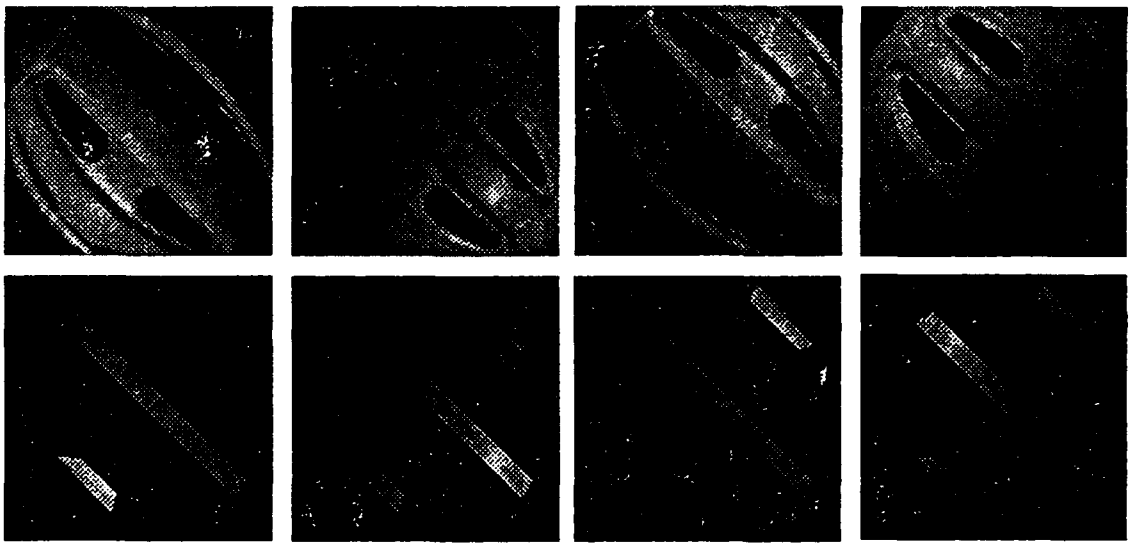

Light One Light Two Light Three Light Four

In addition to interreflection the plastic exhibited a small specular spike. Due to the averaging nature of the pixels in the CCD array, most of the images did not show the spike. However, the image due to light source number two did show the spike. The spike's presence caused the gradient descent fit to not converge, for light source number two's specular lobe. To compensate for the any spike in the other images, we increased the specular threshold in the four light illuminated area to:

$$Rdev > 18 \sqrt{(\frac{\partial}{\partial I1}R1 + \frac{\partial}{\partial I1}R2)^2 \sigma_i^2 + (\frac{\partial}{\partial I2}R1 + \frac{\partial}{\partial I2}R2)^2 \sigma_i^2 + (\frac{\partial}{\partial I3}R1 + \frac{\partial}{\partial I3}R2)^2 \sigma_i^2 + (\frac{\partial}{\partial I4}R1 + \frac{\partial}{\partial I4}R2)^2 \sigma_i^2}$$

With these modifications to our algorithm, we were able to extract the specular lobe's char-

acteristic's for light source one, three, and four.

	Offset	B	K
Specular from light source one	-2.1	36.5	8.4
Specular from light source three	-6.4	49.9	10.1
Specular from light source four	-8.1	41.5	8.3
Average values	-4.2	42.6	8.9

The pixel segmentation for the above images is:

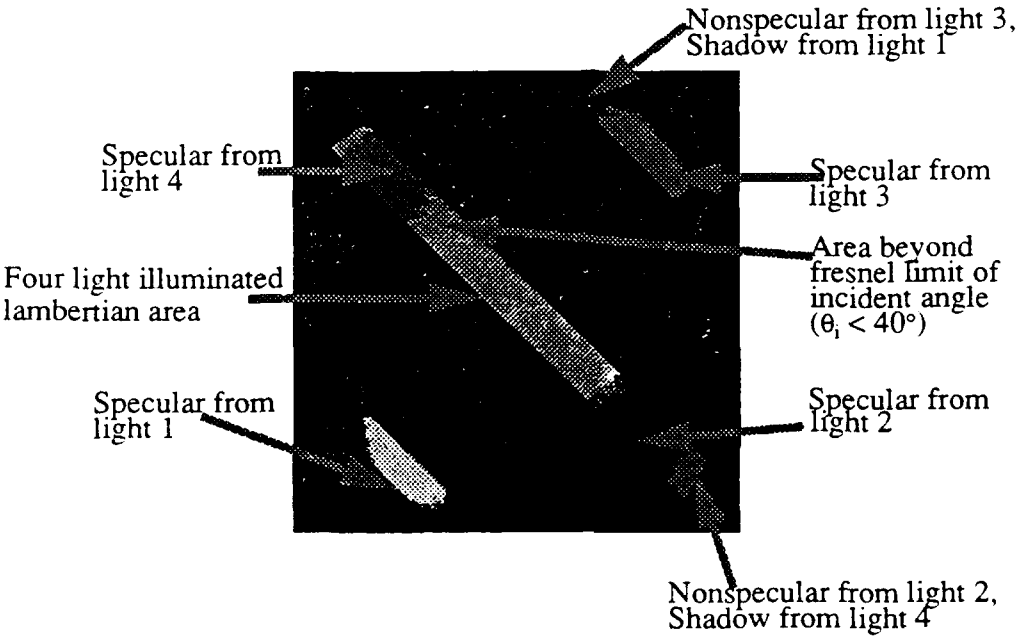

The needle map produced from the four intensity images is:

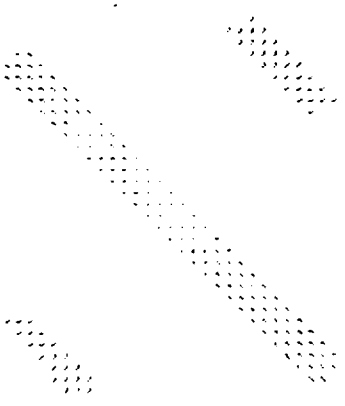

The plot of α^2 versus ln(D*Nz) for light source four is:

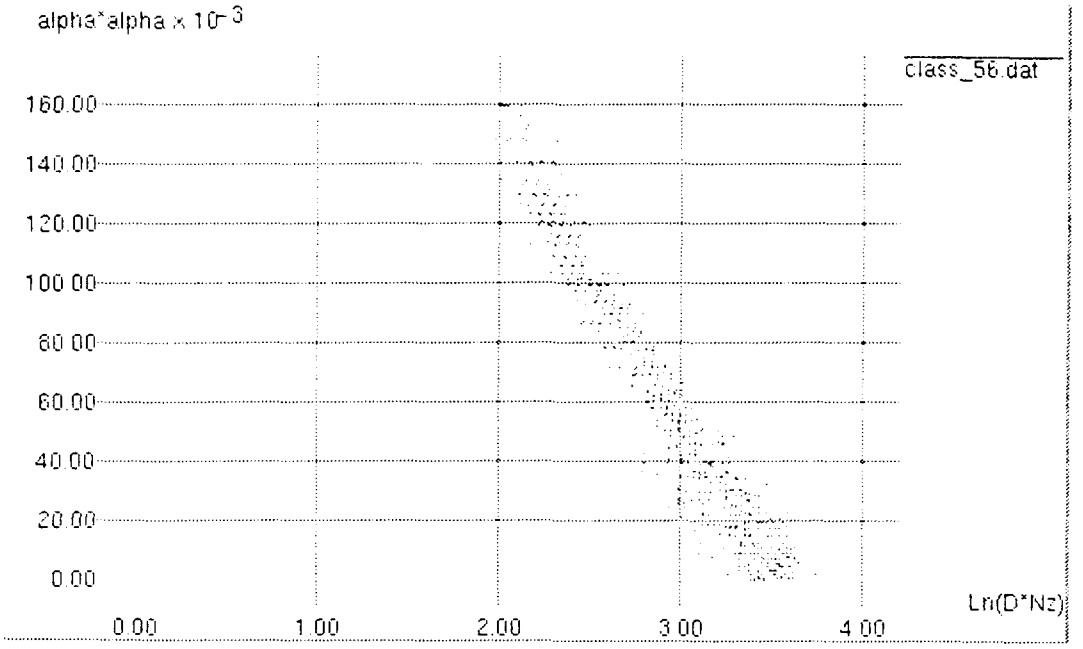

5.2.4. Plastic Bottle

Four images were taken of a plastic bottle. The bottle exhibits a strong specular spike. This prevents us from recovering the roughness of the bottle. However, we are able to recover the shape of the bottle.

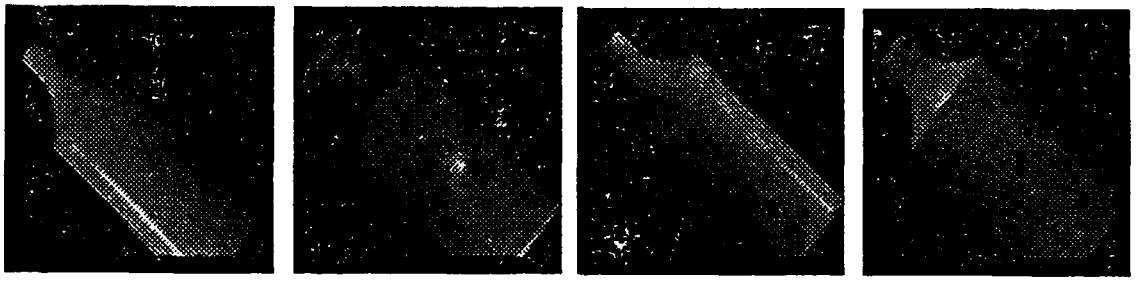

Light One | Light Two | Light Three | Light Four

The pixel segmentation of the four intensity images is:

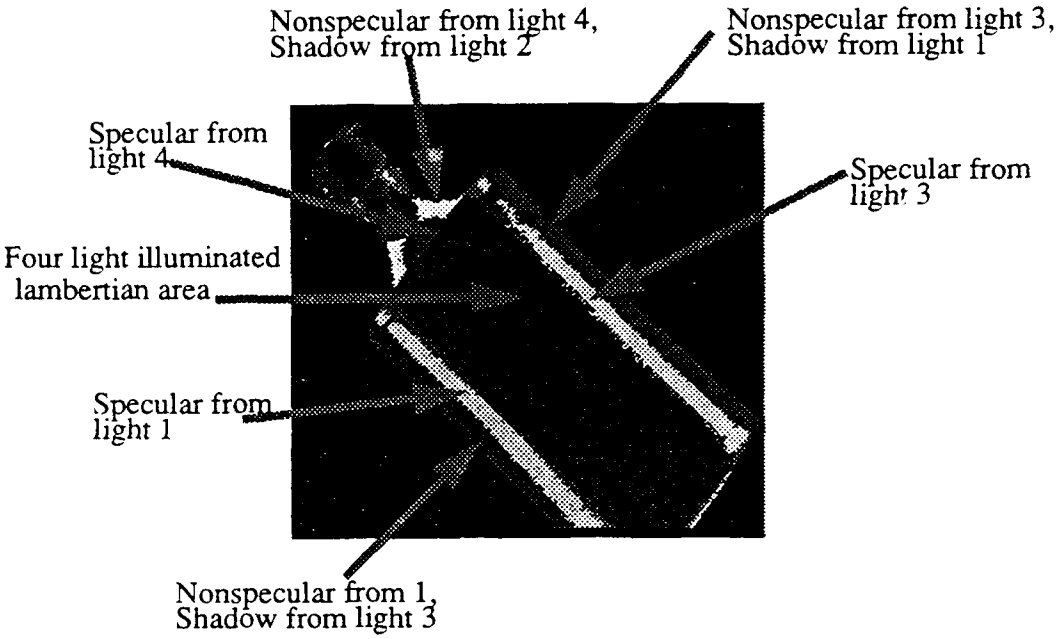

The needle map produced from the four intensity images is:

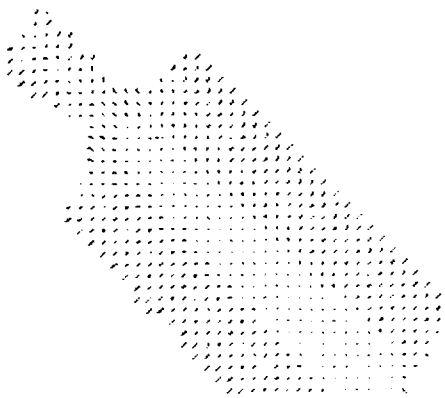

6. Conclusions

We have developed a method for extracting the shape and roughness of surfaces that exhibit a specular lobe. The work includes three important parts: determination of shape, segmentation of pixels into specular and nonspecular pixels, and determination of surface roughness. Coleman and Jain's work for performing segmentation in areas illuminated by four lights, was improved by making the segmentation statistically meaningful. We developed methods for recovering shape and for performing statistical segmentation in regions illuminated by three lights. We also developed methods for recovering shape in regions illuminated by two lights. By examining the illumination conditions in the different regions of the gaussian sphere, we were able to extend photometric stereo to the entire gaussian sphere. Finally, by using a simplified version of the Torrance-Sparrow reflectance model, we were able to develop an algorithm for extracting the specular intensity and surface roughness from specular pixels.

Our methods have been shown to produce reasonable results on synthetic and real images. We have recovered the shape and roughness of objects that exhibit imperfect lambertian albedos, and we have also been able to recover the shape of objects that contain moderate to large specular spikes.

The work has potential application to inspection problems in industrial environments. The roughness extraction algorithms can be used to determine the roughness of objects with a specular lobe. The shape extraction algorithms are fairly robust, and can be applied to objects that exhibit a specular lobe or moderate specular spike.

7. Acknowledgments

The authors would like to thank Kathryn Porsche, Srinivas Akella and Tamara Abell for their constructive suggestions on the manuscript. Eric Krotkov provided help on statistical methods. Carol Novak developed the CMU color chart, and provided instruction on how to use it. We would also like to thank the members of the VASC group at Carnegie Mellon University, who provided many useful suggestions. Fredric Solomon was supported by the IBM Corporation, who is allowing him to study robotics under IBM's Resident Study Program.

8. Appendix A

8.1. Determining Surface Shape With Classical Three Light Photometric Stereo

Photometric Stereo was originally proposed by Woodham. His method uses a stationary camera, three light sources, and a reflectance map for the surface being observed. The reflectance map contains a transformation between surface orientation and image brightness for a given material and light source (direction and intensity). For an arbitrary material, a reflectance map can be built by taking an image of a sphere composed of the material under each of the light sources. Then a simple transformation between the known surface orientation of each point on the sphere and image intensity can be established for each light source.

After the reflectance maps are built, the shape of an unknown surface composed of the same material can be determined. Three images of the unknown surface are taken using the same camera and light sources that were used to build the reflectance maps. Then, a point is found in each of the three reflectance maps that satisfies the measured intensity and possesses a common surface orientation. For three images I1(x,y), I2(x,y), I3(x,y), and their corresponding reflectance maps R1(nx,ny,nz), R2(nx,ny,nz), R3(nx,ny,nz), we need to find a (nx,ny,nz) which satisfies the following set of equations for a given (x,y).

$$I1(x,y) = R1(nx,ny,nz)$$
$$I2(x,y) = R2(nx,ny,nz)$$
$$I3(x,y) = R3(nx,ny,nz)$$

For a lambertian (diffuse) surface, with surface normal, **N**, and light source direction, **S**,

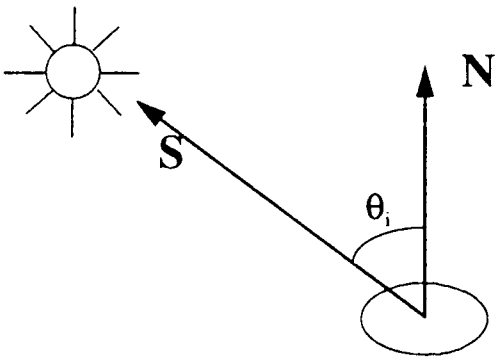

$$I = \rho \cos\Theta_i$$
$$I = \rho(\mathbf{S} \bullet \mathbf{N})$$
$$I = \rho(SxNx + SyNy + SzNz)$$

where ρ is the albedo, θ_i is the incident angle. (Sx, Sy, Sz) and (Nx, Ny, Nz) are the x, y, and z components of the unit source vector, **S**, and unit surface normal vector, N, respectively. The albedo encompasses the light source intensity and relative reflectance of the surface. So, for a lambertian surface, the intensity is just dependent on the light source direction, surface

normal, and the albedo. The intensity is independent of the viewing direction.

Therefore, if the surface is lambertian, we do not need to store an explicit reflectance map. We can determine the surface normal of a point if we know the three light source directions and three intensity values of a point. In matrix form we can write:

$$\begin{bmatrix} S1x & S1y & S1z \\ S2x & S2y & S2z \\ S3x & S3y & S3z \end{bmatrix}^{-1} \begin{bmatrix} I1 \\ I2 \\ I3 \end{bmatrix} = \begin{bmatrix} Nx \\ Ny \\ Nz \end{bmatrix}$$

where S1x, S1y, and S1z are the x, y, and z components of the unit vector to light source number one.

9. References

[1] W. M. Silver, "Determining Shape and Reflectance Using Multiple Images", S.M. Thesis, Dept. of Electrical Engineering and Computer Science, MIT, Cambridge, Massachusetts, June, 1980.

[2] S. K. Nayar, K. Ikeuchi, T. Kanade, "Surface Reflections: Physical and Geometrical Perspectives", *IEEE Trans. of Pattern Analysis and Machine Intelligence*, Vol. 13, No. 7, pp. 611-634, July, 1991.

[3] K. Torrance and E. Sparrow, "Theory for Off-Specular Reflection from Roughened Surfaces", *Journal of the Optical Society of America*, No. 57, pp. 1105-1114, 1967

[4] R. J. Woodham, "Reflectance Map Techniques for Analyzing Surface Defects in Metal Castings", PhD Thesis, Artificial Intelligence Laboratory, MIT, Cambridge, Massachusetts, June, 1978.

[5] K. Ikeuchi, "Determining the surface orientations of specular surfaces by using the photometric stereo method", *IEEE Trans. of Pattern Analysis and Machine Intelligence*, Vol. 3, No. 6, pp. 661-669, November, 1981.

[6] S. K. Nayar, A. C. Sanderson, L. E. Weiss, D. D. Simon, "Specular Surface Inspection Using Structured Highlight and Gaussian Images", *IEEE Trans. on Robotics and Automation*, Vol. 6, No. 2, pp. 208-218, April, 1990.

[7] E. N. Coleman and R. Jain, "Obtaining 3-dimensional shape of textured and specular surfaces using four-source photometry", *Computer Graphics and Image Processing*, Vol. 18, No. 4, pp. 309-328, April, 1982.

[8] G. Healey and T.O. Binford, "Local Shape from Specularity", *Computer Vision Graphics and Image Processing*, Vol. 42, pp. 62-86, 1988.

[9] S. K. Nayar, K. Ikeuchi, T. Kanade, "Determining Shape and Reflectance of Hybrid Surfaces by Photometric Sampling", *IEEE Trans. on Robotics and Automation*, Vol. 6, No. 4, pp. 418-431, August, 1990.

[10] K. Ikeuchi and K. Sato, "Determining Reflectance Parameters Using Range and Brightness Images", CMU-CS-90-106, February, 1990.

[11] P. R. Bevington, "Data Reduction and Error Analysis for the Physical Sciences", McGraw-Hill, New York, 1969, pp. 56-65.